Atmospheric
Measurement
Techniques

Results of a long-term international comparison of greenhouse gas and isotope measurements at the Global Atmosphere Watch (GAW) Observatory in Alert, Nunavut, Canada

Douglas E. J. Worthy[1,★], Michele K. Rauh[1,★], Lin Huang[1,★], Felix R. Vogel[1], Alina Chivulescu[1],
Kenneth A. Masarie[2], Ray L. Langenfelds[3], Paul B. Krummel[3], Colin E. Allison[3], Andrew M. Crotwell[4,9],
Monica Madronich[4,9], Gabrielle Pétron[4,9], Ingeborg Levin[5], Samuel Hammer[5], Sylvia Michel[6], Michel Ramonet[7],
Martina Schmidt[7,5], Armin Jordan[8], Heiko Moossen[8], Michael Rothe[8], Ralph Keeling[10], and Eric J. Morgan[10]

[1]Environment and Climate Change Canada (ECCC), Climate Research Division, Toronto, Ontario, Canada
[2]Skydata Solutions LLC, Boulder, Colorado, USA
[3]Commonwealth Scientific and Industrial Research Organisation (CSIRO), Environment, Aspendale, Victoria, Australia
[4]Cooperative Institute for Research in Environmental Sciences (CIRES), University of Colorado, Boulder, Colorado, USA
[5]Institut für Umweltphysik (UHEI-IUP), Heidelberg University, Heidelberg, Germany
[6]Institute of Arctic and Alpine Research (INSTAAR), University of Colorado, Boulder, Colorado, USA
[7]Laboratoire des Sciences du Climat et de l'Environnement (LSCE), Gif-sur-Yvette, France
[8]Max Planck Institute for Biogeochemistry (MPI-BGC), Jena, Germany
[9]National Oceanic and Atmospheric Administration (NOAA), Earth System Research Laboratory, Boulder, Colorado, USA
[10]Scripps Institute of Oceanography (SIO), La Jolla, California, USA
★These authors contributed equally to this work.

Correspondence: Michele K. Rauh (michele.rauh@ec.gc.ca) and Lin Huang (lin.huang@canada.ca)

Abstract. Since 1999, Environment and Climate Change Canada (ECCC) has been coordinating a multi-laboratory comparison of measurements of long-lived greenhouse gases in whole air samples collected at the Global Atmosphere Watch (GAW) Alert Observatory located in the Canadian High Arctic ($82°28'$ N, $62°30'$ W). In this paper, we evaluate the measurement agreement of atmospheric CO_2, CH_4, N_2O, SF_6, and stable isotopes of CO_2 ($\delta^{13}C$, $\delta^{18}O$) between leading laboratories from seven independent international institutions. The measure of success is linked to target goals for network compatibility outlined by the World Meteorological Organization's (WMO) GAW greenhouse gas measurement community. Overall, based on ~ 8000 discrete flask samples, we find that the co-located atmospheric CO_2 and CH_4 measurement records from Alert by CSIRO, MPI-BGC, SIO, UHEI-IUP, and ECCC versus NOAA (the designated reference laboratory) are generally consistent with the WMO compatibility goals of ± 0.1 ppm CO_2 and ± 2 ppb

CH_4 over the 17-year period (1999–2016), although there are periods where differences exceed target levels and persist as systematic bias for months or years. Consistency with the WMO goals for N_2O, SF_6, and stable isotopes of CO_2 ($\delta^{13}C$, $\delta^{18}O$) has not been demonstrated. Additional analysis of co-located comparison measurements between CSIRO and SIO versus NOAA or INSTAAR (for the isotopes of CO_2) at other geographical sites suggests that the findings at Alert for CO_2, CH_4, N_2O, and $\delta^{13}C$–CO_2 could be extended across the CSIRO, SIO, and NOAA observing networks. The primary approach to estimate an overall measurement agreement level was carried out by pooling the differences of all individual laboratories versus the designated reference laboratory and determining the 95th percentile range of these data points. Using this approach over the entire data record, our best estimate of the measurement agreement range is -0.51 to $+0.53$ ppm for CO_2, -0.09‰ to $+0.07$‰ for $\delta^{13}C$, -0.50‰ to $+0.58$‰ for $\delta^{18}O$, -4.86

to $+6.16$ ppb for CH_4, -0.75 to $+1.20$ ppb for N_2O, and -0.14 to $+0.09$ ppt for SF_6. A secondary approach of using the average of 2 standard deviations of the means for all flask samples taken in each individual sampling episode provided similar results. These upper and lower limits represent our best estimate of the measurement agreement at the 95 % confidence level for these individual laboratories, providing more confidence for using these datasets in various scientific applications (e.g., long-term trend analysis).

1 Introduction

For more than 60 years, scientists have been making high-precision measurements of atmospheric CO_2 (Keeling, 1960). At first, the objective was to understand global features in well-mixed marine air by documenting CO_2 abundance, seasonal patterns, and trends. For this purpose, only a few remote sampling sites were established. Over time the emphasis has shifted to better understand the carbon cycle including emissions to and removal processes from the atmosphere. Today, a global observational network maintained by many laboratories operates high-precision measurements of long-lived greenhouse gases (GHGs) and complementary trace species at hundreds of locations (WMO, 2019, 2022). The measurement community has held regular meetings on measurement technology since 1975, initiated by Charles David Keeling. These meetings are known as "carbon dioxide, other greenhouse gases, and related measurement techniques (GGMT) meetings" and are sponsored by the WMO and International Atomic Energy Agency (IAEA). Proceedings from these meetings are published in Global Atmosphere Watch (GAW) reports (e.g., GAW Report, 2016, 2018, 2020), which are important references for existing and new laboratories. These reports include measurement target recommendations for GHG network compatibility. These targets reflect the scientifically desirable level of network agreement in measurements of well-mixed background air, so the data of different laboratories can be used together in global models or to infer regional GHG fluxes.

Atmospheric measurements of CO_2 and other trace gas species and isotopes are reported by many international laboratories and are often freely available either directly from the originating measurement laboratory (Masarie and Tans, 1995; Masarie et al., 2014; Ramonet et al., 2020; Heimann et al., 2022) or from the WMO World Data Centre for Greenhouse Gases (WDCGG) (https://gaw.kishou.go.jp, last access: 17 November 2023). For nearly 30 years, atmospheric measurements of CO_2 have been used to derive estimates of CO_2 surface fluxes around the globe (Heimann and Keeling, 1989; Tans et al., 1990; Fan et al., 1998; Bousquet et al.,

2000; Gloor et al., 2000; Gurney et al., 2002; Peters et al., 2007; Chevallier et al., 2010; Peylin et al., 2013; Rödenbeck et al, 2018a, b; Friedlingstein et al., 2022). Similar studies have also been carried out for CH_4 (Houweling et al., 2017) and N_2O (Schilt et al., 2010; Thompson et al., 2019). When all available datasets are used in those applications, the users usually assume that these datasets are compatible and consistent over time. However, the applications may be limited by various types of inconsistencies between the datasets, including differences in scales or scale realizations and in sampling systems or procedures, etc. When persistent bias exists between laboratories, the applications such as flux estimates derived by modeling systems using combined datasets on various spatial domains and temporal scales can have large uncertainties (Masarie et al., 2001; Ramonet et al., 2020). To address potential bias, laboratories routinely evaluate measurement traceability and reproducibility within their own laboratory and also compare their measurements with those from other laboratories. Data providers in the measurement community are working hard to include uncertainties with their measurements in order to inform data users. For these reasons, evaluating and quantifying the inconsistencies, biases, or level of agreements for observational records within and between laboratories over time is important.

The widely adopted strategy for assessing the level of agreement of different atmospheric trace gas data records is to conduct ongoing comparisons of the measurements of flask air collected at the same time and the same location (Masarie et al., 2001, 2003; Langenfelds et al., 2003). Based on these previous studies, which involved the comparison of only two laboratories at the same location, this comparison strategy can reveal differences from air sample collection, storage, extraction and analysis, data processing, and maintenance of the laboratory calibration scale, etc. Subtle problems can arise at any step in the measurement procedure. They can occur simultaneously and may exist in one or more of the participating laboratories. Identifying the cause(s) of these inconsistencies often proves difficult (Masarie et al., 2001). Many laboratories often participate in additional comparison experiments designed to help elucidate the cause(s) of observed differences. Laboratories also realize that when comparison results are examined in near-real time, the information can be a valuable quality control measure where problems can potentially be detected and addressed soon after they develop (Levin et al., 2020). A data comparison site administered by NOAA and accessible exclusively to data providers was established for ongoing comparisons in 1999, and it is still in operation today. This platform provides preliminary comparisons for quality control purposes and serves as a good starting point for further in-depth analysis.

The Alert Observatory (ALT), Canada, along with the Mauna Loa Observatory (MLO), USA, and the Cape Grim Observatory (CGO), Australia, are designated as GHG comparison sites by WMO-GAW (GAW Report, 2006), where well-mixed background air can be sampled and measured.

Alert has the most extensive flask comparison program of the three with seven individual flask programs at any time, each focusing on a variety of measurements and respective scientific priorities. In addition, the corresponding comparison results among the three sites (ALT, MLO, and CGO) can provide more information on site-specific inconsistencies and facilitate merging the data records from individual networks.

In this paper, we present the comparison results of atmospheric CO_2, CH_4, N_2O, and SF_6 and the stable isotopes of CO_2 ($\delta^{13}C$, $\delta^{18}O$) measured by the seven international institutions at Alert over the period of 1999–2016. Although some laboratories have measurements prior to 1999 and continue after 2016, this period was chosen because it includes the largest number of laboratories and species measured. The participating institutions are Environment and Climate Change Canada (ECCC), Commonwealth Scientific and Industrial Research Organisation (CSIRO), Max Planck Institute for Biogeochemistry (MPI-BGC), Heidelberg University, Institut für Umweltphysik (UHEI-IUP), Laboratoire des Sciences du Climat et de l'Environnement (LSCE), Scripps Institution of Oceanography (SIO), and the National Oceanic and Atmospheric Administration (NOAA) in collaboration with the Stable Isotope Laboratory at the University of Colorado Institute of Arctic and Alpine Research (INSTAAR). Together with Alert results, we also present corresponding comparisons between CSIRO, SIO, and NOAA at MLO and between CSIRO and NOAA at CGO for the same time period (1999–2016). This is the first report of such a large-scale comparison study. While timely publications of the intercomparison results are desirable, it can be challenging due to the large number of groups involved and ongoing evolving parameters including the adoption of new calibration scales, data corrections, and the limited dedicated resources to carry out these exercises.

2 Methods

2.1 Types of comparison

The commonly used measurement approaches for GHGs and related tracers include (1) discrete flask air samples collected in the field (commonly collected as a pair or as multiple flasks in series or in parallel) and shipped to a measurement laboratory or laboratories for analysis and (2) continuous measurements in situ, conducted using analytical equipment located at the sampling location. The two approaches are complementary, and each approach will remain essential due to their respective advantages and disadvantages. In situ measurements can provide information at very high temporal resolution so that synoptic-scale meteorological events can be observed, which may only by chance be captured by a weekly discrete air sample. In situ monitoring approach requires a physical facility with reliable power, easy access as

well as a high degree of automation, and internet capability to monitor the observation systems remotely. On the other hand, flask air samples are returned to the laboratories with sufficient air, and many laboratories can measure multiple trace gases and their stable isotopes from a single discrete air sample. Also, the relatively low operating cost and minimal infrastructure requirements of flask sampling allows for spatial coverage involving more locations. Many laboratories have opted for an approach including discrete flask-air sampling and, when possible, in situ measurements at one or two key sites to balance temporal and spatial coverage and a suite of measured species.

This study presents two types of discrete flask comparisons, which are known as co-located and same-flask comparisons. The focus is the co-located comparisons, but results from the same-air flask comparisons, as well as same-cylinder (round robins) comparisons, are included to help facilitate the interpretation of the co-located comparison results. These complementary comparisons could reveal cumulative differences due to errors introduced at one or more steps in the entire sampling and measurement process.

Co-located flask air measurement comparison. A co-located comparison generally describes a comparison of two or more measurement records derived using independent collection systems or methods and/or analytical systems at the same location, at approximately the same time and during predefined atmospheric conditions (i.e., wind direction and minimum wind speed requirements). When these conditions are met, observed differences are primarily due to experimental discrepancies instead of changes in the atmospheric signal. Co-located comparisons are designed to evaluate the measurement agreements within or between laboratories due to uncertainties associated with sampling procedures/systems, analytical procedures, data processing, and laboratory calibration scales. Potential errors could arise from any or all of the steps.

Same-flask air measurement comparison. A same-flask air comparison evaluates the independent measurement results when two or more programs or analytical systems measure air from the same "collected sample" container for the same suite of trace species. Typically, the same-flask air comparison sample is shipped from the remote sampling location to the closest participating laboratory or to the laboratory with lowest sample consumption. This same-flask sample is then shipped to a second participating laboratory for analysis. Additional laboratories or analytical systems could further analyze the sample, provided there is sufficient air remaining in the flask, although the risk of sample contamination or alteration may increase. A same-flask comparison experiment evaluates the measurement agreement within or between laboratories caused only by measurement and data processing steps and not by sample collection procedures/systems. A problem during sample collection, such as contamination, could still potentially affect the air in the flask, but this should not impact the comparison results for same-flask analysis.

Typically, only one flask of a pair is analyzed by both labs, thereby providing information whether the analysis procedure by one of the labs has caused contamination or altered the composition of the air in the flask. The reference laboratory for same-flask comparisons at Alert is ECCC.

Same-cylinder air measurement comparison. A same-cylinder air measurement comparison refers to an experiment in which two or more laboratories measure air in a pressurized cylinder for the same suite of trace species and then compare the independent measurement results. Like the same-flask air comparison experiment, the same-cylinder air comparison evaluates the measurement agreements within or between laboratories involving the overall uncertainties from analytical procedures (i.e., extracting air from the cylinder, introducing the aliquot of air into their detection system, measuring the sample) to processing the results and maintaining their laboratory calibration scales. Because the volume of air sample in a pressurized cylinder is orders of magnitude greater than that in a flask, many more laboratories can participate in the comparison, and each laboratory can make multiple measurements thereby obtaining an optimized measurement uncertainty. One drawback of the same-cylinder comparison is the added time and expense of shipping pressurized cylinders, which can be subject to strict international safety regulations. Consequently, the frequency for this type of comparison is from quarterly, at best, to every few years and the results only represent a snapshot in time. It should be noted that analyzers used to measure flask samples are not necessarily the same instruments that are used for cylinder air analysis in each laboratory, and this can contribute uncertainty and possibly bias to the comparison. It is important in these types of comparisons that at least one laboratory, generally the coordinating laboratory, measures the air before and after any other laboratories to characterize/quantify any composition changes that may have occurred during the period of comparison. In addition, it is important to note that drifts in concentrations may occur with cylinder depressurization.

The WMO/IAEA "Round Robin" (RR) Comparison Experiment, administered by NOAA, is one example of a same-cylinder air comparison experiment. This experiment is designed to assess the level of agreement within the participating laboratories and assess their ability to maintain links to the WMO mole fraction scales for CO_2, CH_4, and other trace gas species. There have been seven WMO/IAEA Round Robin experiments since it was first introduced in 1974; the most recent experiment started in November of 2020, includes participation by 59 laboratories (Global Monitoring Laboratory – Carbon Cycle Greenhouse Gases (https://gml. noaa.gov/ccgg/wmorr/, last access: 17 November 2023)), and is still ongoing. Round robin results from RR nos. 5 and 6 from the participating laboratories are included in certain figures and in Table S1 in the Supplement, if the results are on the same scale as the data used in this analysis.

2.2 The Alert Dr. Neil Trivett Global Atmosphere Watch Observatory

Alert, Nunavut, is located on the northern tip of Ellesmere Island in the Canadian High Arctic ($82°28'$ N, $62°30'$ W) far from the major industrial regions of the Northern Hemisphere. Alert is the site of a military station, Canadian Forces Station (CFS) Alert, and an ECCC Upper Air Weather Station. The Alert Dr. Neil Trivett Global Atmosphere Watch (GAW) Observatory (ALT) is located 6 km south of CFS Alert on a plateau 210 m above sea level. The land around Alert is covered with snow for almost 10 months of the year and has a sparse covering of polar desert vegetation in the summer. The degree of contamination from the local environment is minimal, with winds originating from within the ENE sector, which includes CFS Alert camp (Worthy et al., 1994), less than 4 % of the time. The ALT observatory is ideally situated for monitoring well-mixed air masses representative of very large spatial extent in the Northern Hemisphere. ALT has been the cornerstone of ECCC's atmospheric research program since 1975, and in 1986 it was officially designated a WMO-GAW Global Observatory. The observatory was officially renamed the Dr. Neil Trivett Global Atmosphere Watch Observatory in 2006. With its existing infrastructure and strong multi-laboratory research activity, ALT is well positioned to support a multi-laboratory co-located atmospheric comparison experiment.

2.3 Flask sampling at ALT, MLO, and CGO

2.3.1 Sampling timelines

The species measured, types of comparisons (co-located/same flask), and timelines of comparison experiments conducted at Alert from 1999–2016 are summarized in Table 1. Individual laboratory participation and species measured were not consistent over the entire 17-year period. For example, ECCC's program for CO_2 isotopes was terminated in December 2009, and LSCE's program for all trace gases and isotopes was discontinued in September 2013. The same flask air comparison program for all trace gases at Alert has an end date of December 2013.

At MLO and CGO, co-located flask sampling was conducted by CSIRO, SIO, and NOAA for the same species and similar time periods as ALT.

2.3.2 Sampling systems

Table 2a describes the sample collection system at ALT for each laboratory, including flask type, sampling frequency, and apparatus used during the specified time period. Most laboratories at ALT used double-stopcock flasks, which allow for flow-through flushing prior to filling to an overpressure of 5 to 15 psi. Exceptions include SIO, who used single-stopcock and evacuated flasks, and CSIRO, who used some single-stopcock pressurized flasks from 1999 to 2003. Air

Table 1. Summary of available observations and flask comparison types for each participating laboratory during the period of this study at ALT.

LAB	TYPE OF ICP		Species
ECCC	CO-LOCATED	CO_2, CH_4, N_2O, SF_6 $\delta 13C$, $\delta 18O$	
	SAME-FLASK	CO_2, CH_4, N_2O, SF_6 $\delta 13C$, $\delta 18O$ with MPI-BGC $\delta 13C$, $\delta 18O$ with CSIRO	
CSIRO	CO-LOCATED	CO_2, CH_4, N_2O $\delta 13C$, $\delta 18O$	
	SAME-FLASK	CO_2, CH_4, N_2O $\delta 13C$, $\delta 18O$	
NOAA	CO-LOCATED	CO_2, CH_4, N_2O, SF_6 $\delta 13C$, $\delta 18O$	
	SAME-FLASK	CO_2, CH_4, N_2O, SF_6	
SIO	CO-LOCATED	CO_2 $\delta 13C$, $\delta 18O$	
	SAME-FLASK		
UHEI-IUP	CO-LOCATED	CO_2, CH_4, N_2O $\delta 13C$, $\delta 18O$	
	SAME-FLASK	CO_2, CH_4, N_2O	
MPI-BGC	CO-LOCATED	CO_2, CH_4, N_2O, SF_6 $\delta 13C$, $\delta 18O$	
	SAME-FLASK	CO_2, CH_4, N_2O, SF_6 $\delta 13C$, $\delta 18O$	
LSCE	CO-LOCATED	CO_2, CH_4, N_2O, SF_6 $\delta 13C$, $\delta 18O$	
	SAME-FLASK	CO_2, CH_4, N_2O, SF_6	

(Year columns span 1999–2016 with bars indicating data availability per laboratory.)

was typically dried using a cryocooler before filling by most laboratories, except SIO and NOAA, who did not dry their air samples either by a cryocooler or by a chemical dryer, and MPI-BGC, who used a $Mg(ClO_4)_2$ dryer until 2015 before switching to a cryocooler. Sampling was conducted at a height of 10 m, except SIO and NOAA, whose intakes were roughly 2 and 5 m, respectively.

At MLO, SIO's sampling was the same as ALT, but CSIRO's sampling used a chemical dryer instead of a cryocooler and had a 40 m air intake. NOAA's sampling was similar to ALT, but some samples were also taken via an undried flow from their in situ system (40 m) (Conway et al., 1994; Dlugokencky et al., 1994).

At CGO, CSIRO's sampling used a chemical dryer from 1999 to 2014 and then switched to a cryocooler and new sampling system. NOAA's sampling at CGO was partially dried, in contrast to being undried at Alert. Samples from both laboratories were taken from 70 m heights (Francey et al., 2003, and Langenfelds et al., 2023). Table 2b outlines the various differences between sampling at ALT, MLO, and CGO for CSIRO, SIO, and NOAA.

Further details about the sampling procedures of all laboratories can be found in the Supplement. Notable impacts of certain sampling parameters on the results are mentioned in the "Results and discussion" (Sect. 3).

2.3.3 Sampling conditions

Table 3 provides the coordinated ALT weekly flask air collection schedule for participating laboratories. The coordinated sampling schedule was devised to ensure that the flask samples for each individual laboratory are collected on the same day and as close in time as possible, within a 2 h window. Small variations in sampling time are unlikely to result in notable discrepancies. Flask air samples were collected at Alert during persistent southwesterly wind conditions, when wind speeds were greater than $1.5\,\mathrm{m\,s^{-1}}$ for several hours prior to sample air collection. If conditions were unsuitable on the regular sampling day (Wednesday), sampling would be postponed to the following day. If conditions remained unfavorable by Friday, sampling would proceed, but it was acknowledged that conditions were suboptimal.

At MLO, sampling for all laboratories (NOAA, CSIRO and SIO) was conducted within an hour of each other and prior to noon (local time) in an effort to avoid upslope, non-baseline wind conditions at the site.

At CGO for NOAA and CSIRO, sampling was predominantly carried out under baseline conditions of 190–280° N wind direction and wind speeds exceeding $5\,\mathrm{ms^{-1}}$ wind speed, or the data were subsequently filtered for baseline conditions.

2.4 Instrumentation and analytical methods

Instrumentation and methods used to measure the flask air samples collected at the sampling sites vary between the laboratories and continue to evolve within each laboratory. To the extent possible, each laboratory handles the flask air samples and measurements in the same way as other flasks from their observing network. Table 4 summarizes each laboratory's analytical instrumentation and calibration scales used for each species, for the period of this study. A brief summary of the instrumentation is provided below, and calibration scales will be discussed in more detail in "Results and discussion" (Sect. 3).

For CO_2, all laboratories except for NOAA and SIO used gas chromatography (GC) equipped with a nickel catalyst and flame ionization detector (FID) for the analysis of CO_2 in the flask air samples. The nickel catalyst converts CO_2 in the sample to CH_4, permitting analysis of CO_2 using the FID. NOAA used non-dispersive infrared (NDIR) spectroscopy throughout, and SIO used an NDIR until 2012 and then switched to a cavity ring down (CRDS) analyzer. The GC, NDIR, and CRDS systems have comparable analytical precision, ranging between 0.01 ppm (CRDS) and 0.05 ppm (GC).

For stable isotope ratio measurements of atmospheric CO_2, all participating laboratories used isotope ratio mass spectrometry (IRMS). Before introduction of the sample into an IRMS, the CO_2 in the air sample is first extracted using either an offline glass vacuum extraction system to prepare samples for later analysis (Bollenbacher et al., 2000; Huang

Table 2. (a) Summary of flask type, sampling frequency, and apparatus used for each participating laboratory during the period of this study at ALT. **(b)** Differences of sampling between ALT, MLO, and CGO.

(a)

Group	Flask type	Sampling frequency	Filling apparatus	Sample drying	Inlet height
CSIRO	1999–Nov 2014* ECCC flasks Nov 2014–present CSIRO 0.5 L pressurized double valves Teflon (PFA) O-rings *see Supplement for details	variable see Supplement for details	1999–Aug 2016 SIO sampler Aug 2016–present CSIRO/UHEI/ ECCC sampler	cryocooler	10 m tower
MPI-BGC	2005–present 1 L pressurized double valves PCTFE O-rings	triplet bi-weekly	MPI-BGC sampler	2005–2015 $Mg(ClO_4)_2$ 2015–present cryocooler	10 m tower
UHEI-IUP	2005-present 1 L pressurized double valves PCTFE O-rings	1 pair weekly	2005–Aug 2016 SIO sampler 2016–present CSIRO/UHEI/ ECCC sampler	cryocooler	10 m tower
LSCE	2007–2013 1 L pressurized double valves PCTFE O-rings	1 pair weekly	LSCE sampler	cryocooler	10 m tower
SIO	1999–present 5 L evacuated single valve greased	1 pair weekly	N/A	None	arm's length above head
ECCC	1999–present 2 L pressurized double valves Viton O-rings	1 pair weekly	1999–Aug 2016 SIO sampler 2016–present CSIRO/UHEI/ ECCC sampler	cryocooler	10 m tower
NOAA	1999–present 2.5 L pressurized double valves PTFE Teflon O-rings	1999–2011 2 pairs weekly 2011–present 1 pair weekly	portable sampling unit (PSU)	none	5 m sample line extending from sampler

(b)

Group	ALT	MLO	CGO
CSIRO	different flask types SIO O_2/N_2 sampler cryocooler, 10 m,	CSIRO 0.5 L flasks flask pump unit (FPU) $Mg(ClO_4)_2$, 40 m,	CSIRO 0.5 L flasks FPU (1999–2014), $Mg(ClO_4)_2$; Sherpa unit (2014–2016), cryocooler, 70 m,
SIO	undried, ~ 2 m	undried, ~ 2 m	N/A
NOAA	portable sampler unit (PSU), undried, 5 m	PSU, undried, 5 m; also some flasks from in situ air stream, undried, 40 m	PSU, partially dried using a condenser, 70 m

Table 3. Flask air collection schedule for each participating laboratory at ALT.

Week	Indoor flasks	Typical times (UTC)	Indoor flasks (other)	Typical times (UTC)	Outdoor flasks	Typical times (UTC)
1	ECCC (1 pair weekly)	14:00–14:30	MPI-BGC (triplet bi-weekly)	14:15–14:45	NOAA (1 pair weekly)	14:05–14:15
	CSIRO (1 pair as below*)	14:30–15:00	LSCE (1 pair weekly)	14:45–15:15	SIO (1 pair weekly)	14:05–14:10
	UHEI-IUP 1 (pair weekly)	15:00–15:30				
2	ECCC 1 (pair weekly)	14:00–14:30	LSCE (1 pair weekly)	14:15–14:45	NOAA (1 pair weekly)	14:05–14:15
	UHEI-IUP (1 pair weekly)	14:30–15:00			SIO (1 pair weekly)	14:05–14:10

* CSIRO: biweekly from Nov to May; weekly rest of the year.

Table 4. Summary of types of instrumentation, repeatability, and scales used for the flask air analysis at each participating laboratory during the period of this study.

Laboratory	Species	Duration of instrument use	Instrument type	Calibration scale
CSIRO	CO_2, CH_4	1999–2016	GC-FID[1]	X2007, X2004A
	N_2O	1999–2016	GC-ECD[2]	X2006A
	$\delta^{13}C$ and $\delta^{18}O$-CO_2	1999–2016	IRMS[3]	Local (see Table 5)
MPI-BGC	CO_2, CH_4, N_2O, SF_6	2005–2016	GC-FID[4]/GC-ECD[4]	X2007, X2004A, X2006A, X2014
	$\delta^{13}C$ and $\delta^{18}O$–CO_2	2005–2016	IRMS[3]	Local JRAS-06 (see Table 5)
UHEI-IUP	CO_2, CH_4, N_2O	2005–2016	GC-FID[4]/GC-ECD[4]	X2007, X2004A, X2006A
	$\delta^{13}C$ and $\delta^{18}O$–CO_2	2005–2016	IRMS[3]	Local (see Table 5)
LSCE	CO_2, CH_4, N_2O, SF_6	2007–2013	GC-FID[4]/GC-ECD[4]	X2007, X2004A, X2006A, X2014
	$\delta^{13}C$ and $\delta^{18}O$–CO_2	2007–2013	IRMS[3]	Local (see Table 5)
SIO	CO_2	1999–2012	NDIR[5]	X08A
		2012–2016	CRDS[6]	X08A
	$\delta^{13}C$ and $\delta^{18}O$–CO_2	1999–2000	IRMS[7]	Local (see Table 5)
		2000–2016	IRMS[8]	Local (see Table 5)
ECCC	CO_2	1999–2006	NDIR[9]	X2007
	CO_2, CH_4, N_2O, SF_6	1999–2016	GC-FID[4]/GC-ECD[4]	X2007, X2004A, X2006A, X2014
	$\delta^{13}C$ and $\delta^{18}O$–CO_2	1999–2009	IRMS[3]	Local (see Table 5)
NOAA/ INSTAAR	CO_2	1999–2016	NDIR[10]	X2007
	CH_4, N_2O, SF_6	1999–2016	GC-FID[4]/GC-ECD[4]	X2004A, X2006A, X2014
	$\delta^{13}C$ and $\delta^{18}O$–CO_2	1999–2016	IRMS[8]	Local JRAS-06 (see Table 5)
		2005–2016	IRMS[11]	Local JRAS-06 (see Table 5)

[1] Carle 400 (repeatability of 0.05 ppm for CO_2, 3 ppb for CH_4). [2] Shimadzu (repeatability of 0.2 ppb for N_2O). [3] MAT252 (repeatability of 0.02 ‰ for $\delta^{13}C$–CO_2 and 0.04 ‰ for $\delta^{18}O$–CO_2). [4] Agilent 5890/6890/7890 (repeatability of 0.05 ppm for CO_2, 3 ppb for CH_4, 0.2 ppb for N_2O, and 0.04 ppt for SF_6). [5] APC model 55 (repeatability of 0.05 ppm for CO_2). [6] Picarro (repeatability of 0.01 ppm for CO_2). [7] VGII (repeatability of 0.02 ‰ for $\delta^{13}C$–CO_2 and 0.04 ‰ for $\delta^{18}O$–CO_2). [8] Micromass Optima DI (repeatability of 0.02 ‰ for $\delta^{13}C$–CO_2 and 0.04 ‰ for $\delta^{18}O$–CO_2). [9] Siemens Ultramat (repeatability of 0.05 ppm for CO_2). [10] Licor (repeatability of 0.05 ppm for CO_2). [11] GV IsoPrime DI (repeatability of 0.02 ‰ for $\delta^{13}C$–CO_2 and 0.04 ‰ for $\delta^{18}O$–CO_2).

et al., 2013) or using an online metal vacuum extraction system coupled directly to the mass spectrometer (Trolier et al., 1996; Werner et al., 2001; Allison and Francey, 2007) for analysis within 1 h of CO_2 extraction. All laboratories except ECCC and SIO used an online extraction approach; ECCC and SIO used an offline technique where pure CO_2 samples were flame-sealed in ampoules after extraction and stored for variable lengths of time, ranging from 1 month to 1 year before IRMS analysis (it has been verified at ECCC that the isotopic compositions of CO_2 in ampoules do not change within the range of accepted uncertainty during a storage time of > 10 years). All the laboratories used dual-inlet mode for

$\delta^{13}C$ and $\delta^{18}O$ measurements but employed different strategies to link the individual sample measurements to the primary scale VPDB–CO_2. Table 5 details the various calibration strategies used and highlights the differences that exist between the laboratories. Since 2015, the WMO-GAW community has endorsed the JRAS-06 realization (Wendeberg et al., 2013; GAW Report, 2011) of the VPDB–CO_2 scale for reporting stable isotope measurements of atmospheric CO_2, but this has not been fully implemented by all laboratories. For further explanations of VPDB–CO_2 and JRAS-06, please see Sect. 3.2. For each laboratory, the repeatability of $\delta^{13}C$–CO_2 and $\delta^{18}O$–CO_2 measurements are typically less than $0.02\,‰$ and $0.04\,‰$ (1σ), respectively.

For CH_4, all participating laboratories used gas chromatography (GC) with flame ionization detection (FID) for analysis of CH_4, with typical analytical repeatability of less than 3 ppb. For N_2O and SF_6, all participating laboratories used gas chromatography (GC) equipped with an electron capture detector (ECD) for analysis of N_2O and SF_6 in the weekly collected flask air samples. The analytical repeatability for N_2O and SF_6 using GC–ECD is typically 0.2 ppb and 0.04 ppt respectively.

2.5　Data preparation

All measurements used in this study have been screened by the originating laboratory to ensure that each sample and subsequent measurement have not been compromised during collection, storage, and analysis. Each laboratory determines their own criteria for the quality control of their data and assigns the flags "valid", "invalid", or "suspected". These data files were provided to us by individual laboratories and have specific time stamps, which can be found in the Supplement and Table S2. These time stamps identify the state of the data used in this study, in terms of scale updates/corrections, etc., which is important information because the same datasets may be found in other data repositories as updated versions with scale changes and/or modifications. As the data preparation is critical to the results, we describe the detailed methods for data preparation used in this study in the following sections.

Data matching and reference time series. To match the appropriate co-located and same-flask measurements from the seven laboratories for comparison, participants agreed to submit measurement results that include information on sample collection time (in coordinated universal time (UTC)), collection method, flask identification, measurement value, quality control flag, and analytical instrument identification. Matching algorithms identify and separate same-flask measurements (samples with identical collection date/time and container ID) from co-located measurements. All data that have been flagged as "valid" by each individual laboratory are used.

All same-flask measurements from ALT are differenced from measurements by ECCC, on a one-to-one basis (i.e.,

laboratory minus ECCC). All co-located flask measurements from ALT, CGO, and MLO are differenced from the reference time series of NOAA for CO_2, CH_4, N_2O, and SF_6 and INSTAAR for $\delta^{13}C$ and $\delta^{18}O$ of CO_2 (laboratory minus NOAA or INSTAAR). Ideally, the reference time series should demonstrate consistency over the entire comparison period, have minimal gaps, and accurately represent the true abundance of the atmospheric trace gas constituents at the sites. In practice we do not have a single laboratory who we know to be the truth, so we must choose one that best meets our requirements. NOAA and INSTAAR were chosen because their records span the entire period of our study with minimal data gaps. Also, by hosting the WMO Central Calibration Laboratory for CO_2, CH_4 and N_2O, NOAA is well placed to assess measurements on the WMO scales and INSTAAR, by virtue of their close association, is an appropriate choice for the stable isotopes of CO_2. Further, NOAA/INSTAAR has extensive and well-documented quality control procedures in place to ensure internal consistency of its measurements (Conway et al., 1994; Dlugokencky et al., 1994; Trolier et al., 1996).

Co-located data pool and analyses. Prior to any ALT, CGO, and MLO co-located analyses, data pools were created for each site and species, consisting of no more than two valid measurements from each laboratory (including NOAA and INSTAAR) for each day of sampling (sampling episode). Since most participants collect a pair of air samples during each sampling episode, two measurement results are typically available. When more than two valid measurements exist for a given sampling episode from a laboratory, we select two at random from the set of available measurements. For example, three (and sometimes four) MPI-BGC flask air samples are collected during each sampling episode at Alert, so two measurements are selected at random from the available valid MPI-BGC measurements and added to the data pool. If there is only one valid measurement available from one of the laboratories, we do include that single sample in the data pool. This data pool process allows for a more equal representation for all laboratories. The first analysis performed using the ALT data pool was the calculation of mean flask pair differences for CO_2, $\delta^{13}C$–CO_2, $\delta^{18}O$–CO_2, CH_4, N_2O, and SF_6 for each participating laboratory, and these can be found in Tables S3 to S8. These flask pair differences could be used as a proxy of individual lab uncertainties. The discussion of these differences will be found in future sections.

For all sites, each laboratory's individual data points in the pool are differenced from the reference time series data in the same pool (i.e., NOAA or INSTAAR). In most cases, the reference time series has two data points, which are averaged and that value is then differenced from each point of the other laboratory. If the reference time series has only one data point for a certain sampling episode, that single point is used for each point of the other laboratory. Our co-located comparison strategy produces a set of difference time series (labo-

Table 5. Summary of $\delta^{13}C$–CO_2 and $\delta^{18}O$–CO_2 scale propagation and calibration strategies employed by each participating laboratory.

	CSIRO	MPI-BGC	UHEI-IUP	SIO	INSTAAR	ECCC
Realization of VPDB–CO_2 scale	Local*	Local (JRAS-06)	Local	Local	JRAS-06	Local
Realization approach and frequency	Calibration of pure CO_2 was done in 1987, 1994 and 2009 using NBS19 and transferred to a suite of CO_2-in-air standards that are independently maintained. The value assignment is consistent with the MPI-BGC scale for d13c.	Calibration was done at the time of implementation and is maintained by various high pressure air cylinders since then.	About once per year. Transfer to internal pure CO_2 gases (Oberlahnstein and Pflanzenstandard) used for daily MSP calibration	A calibration was done in 1994 and maintained CO_2-in-air standards since	Current/recent CO_2-in-air standards measured against MPI-BGC standards on JRAS-06. Previous standards tied through "linking standards"	Once per year since 2001 via NBS19, NBS18, and two lab-carbonate standards (Cal1 and 2) measured together against the same CO_2 working reference
Primary reference material	NBS19	NBS19	Pure CO_2: RM8562, 8563, 8564	Carbonates: NBS19; Pure CO_2: NBS16,17;	NBS19 via JRAS-06 cylinders	Carbonates: NBS19 and NBS18
^{17}O correction	Brand et al. (2010)	Santrock et al. (1985) with IUPAC-recommended values for "lambda" and "κ" coefficients (Brand et al., 2010).	Santrock et al. (1985) (with coefficients $= 0.5$ and $k = 0.008335$)	Craig (1957)	Brand et al. (2010)	Craig (1957)/Allison et al. (1995)
N_2O correction	Mook and Jongsma (1987) using measured CO_2 and N_2O amount fractions.	Ghosh and Brand (2004)	Mook and Jongsma (1987) with measured N_2O	Mook and Jongsma (1987) with estimated N_2O	Mook and Jongsma (1987) with measured N_2O	Mook and Jongsma (1987) with measured N_2O
Scale contraction correction	Explicitly monitored, small, and measurements corrected.	Monitored, negligible, no correction applied	Monitored, negligible, no correction applied		Monitored by surveillance cylinders, negligible due to identical treatment, not corrected for	Monitored, negligible, no correction applied
QA/QC	Suite of surveillance cylinders. Use of air standards also corrects for uncorrected for variability.		Suite of surveillance cylinders		Suite of surveillance cylinders	Regularly daily monitoring during analysis using the ECCC "Big Delta" method, i.e., the relative difference between the two lab carbonates
References	Allison and Francey (2007)	Wendeberg et al. (2011) and references therein	Neubert (1998)	Guenther et al. (2001), Bollenbacher et al. (2000), Lueker et al. (2020)	Trolier et al. (1996), Michel (2022)	Huang et al. (2013)

* A realization of VPDB via an MPI-BGC value-assigned tank and revisions to all CSIRO data is in progress.

ratory minus reference) for each individual trace gas species and isotope measurement record. Before analyzing the time series, we first examined characteristics of their distributions and found that, in general, they are not normally distributed (non-parametric). The statistical approach carried out in this study is based on the assumption of non-normal distributions. It is quite common to observe a pattern of systematic differences (bias) that can be persistent for many months and then change either abruptly or gradually into a different pattern. Thus, we summarize each distribution of individual differences using annual median values with an estimate of the 95 % confidence interval (CI), which makes no assumptions about the distribution of the "true" difference population. The 95 % CI is computed using methods described by Campbell and Gardner (1988). In this way, our initial statistics should not be unduly influenced by outliers. The final derived annual median deviations are compared to the target goals outlined by the WMO-GAW greenhouse gas program to assess the level of agreements of individual datasets with the reference laboratory.

2.6 Level of agreement between multiple measurement records

In addition to the assessment of individual laboratory co-located comparisons, we attempt to estimate the overall level of grouped agreement from multiple measurement records for each species using two approaches. The first approach provides the 95th percentiles of the individual differences of all laboratory's measurements relative to NOAA's or INSTAAR's corresponding observation. However, because variations in NOAA's or INSTAAR's observational records might impact the results, we also report a second proxy for the level of grouped agreement, i.e., 2 standard deviations (2σ) from the means of each weekly sampling episode, which would define a region that includes 95 % of all the measurement values. Although less susceptible to bias by NOAA or INSTAAR, this grouped proxy is also not ideal because the introduction of new programs could potentially alter the mean and hence the 2σ of the group. In addition, the use of 2σ values is less reliable than using percentiles for skewed distributions. But by providing both measures for the level of agreement, we hope that any limitation of one measure over the other can be compensated when interpreting them together. The values determined by both methods reflect the overall maximum bias between the measurement records from multiple monitoring programs.

2.7 Data visualization

For each trace gas and isotope comparison, we have prepared one figure (Figs. 1–6), consisting of several graphs each. For CO_2, $\delta^{13}C$–CO_2, $\delta^{18}O$–CO_2, CH_4, and N_2O, the figures include five graphs each, from (a) to (e), but for SF_6 there are only four graphs labeled (a) to (d). These figures, along

with three data summary tables, are designed to facilitate visualizing and interpreting our results. Graph (a) in these figures displays the time series of each laboratory's measurements. It highlights the long-term trend, seasonal patterns, and natural variability in the records and provides context for the comparison results. Graph (b) consists of several panels, each showing the individual co-located measurement difference (laboratory minus reference) for each laboratory. Differences exceeding the graph's y axis range are plotted with an "X" symbol; however, these data points are still included in all analysis procedures. The dark shaded band, which is also shown in graphs (c)–(e), represents the WMO-GAW-recommended target of measurement agreement for well-mixed air at remote sites in the Northern Hemisphere. Results from past WMO/IAEA Round Robin experiments (Global Monitoring Laboratory – Carbon Cycle Greenhouse Gases (https://gml.noaa.gov/ccgg/wmorr/index.html, last access: 17 November 2023)) are plotted as differences (laboratory minus NOAA or INSTAAR) with yellow triangles, representing each laboratory's level of consistency with the reference lab on scale at the time of the experiment. Table S1 shows round robin differences versus NOAA or INSTAAR for all laboratories over the time period (only RR data that are on the same scale as data in the paper have been included). Graph (c) shows, for each laboratory, the annual medians of the differences plotted in graphs (b) with the lower and upper limits of estimated 95 % confidence intervals (CI). The fourth graph, Graph (d), for all species except SF_6, shows the same analysis as that done at Alert in graphs (c) but for the co-located comparison experiments between SIO, CSIRO, and NOAA at MLO and between CSIRO and NOAA at CGO. Graph (d) for SF_6 is the same as Graph (e) for the others, which shows the individual co-located measurement difference (laboratory minus reference) for all the laboratories as a collective. The blue line shows annual values of 95th percentile ranges (2.5th and 97.5th), and the pink line shows annual means of 2σ for the weekly sampling episodes. For comparison purposes, we have included the annual means, shown in yellow, of the 2σ for the combined weekly sampling episodes between CSIRO, SIO, and NOAA at MLO.

In addition to the main figures and tables, supplementary figures and tables are included for some species when applicable.

3 Results and discussion

As we consider results from 17 years of comparison experiments at Alert, a practical indicator of success is if the measurement agreement reported here falls within the WMO-GAW-recommended target levels for network consistency based on well-mixed background air records (GAW Report, 2020). In other words, it could be assumed that using these records together would not introduce significant uncertainties, if the agreement between independent Alert atmospheric

records is consistently within the WMO-GAW measurement agreement goal over the study period.

In this work, we assess the level of agreement for those individual measurement records at Alert by evaluating the differences related to the reference time series and evaluate these differences as annual and overall median values. When persistent differences exceed the WMO-GAW-recommended targets, we then consider results from same-flask and same-cylinder experiments to confirm the differences if data are available. To support the results at Alert, the corresponding comparisons at MLO and at CGO are also evaluated.

We recognize that, for some species, the network comparison goals may not be currently achievable within current measurement and/or scale transfer uncertainties and that these goals are targeted for application areas which require the smallest possible bias among different datasets for the detection of small trends and gradients. However, there are, of course, other application areas where such tight comparison goals may not be required, such as in urban emission estimates, long-term trend analysis, as well as in some regional modeling studies where uncertainties in air transport, for example, overshadow measurement uncertainties. Our work in this study could provide more confidence on the uncertainty estimation for these applications as well.

3.1 CO_2

All measurements are reported in this paper relative to the WMO X2007 CO_2 mole fraction scale (Zhao and Tans, 2006), except for those from SIO, which are reported on the SIO X08A scale (Keeling et al., 2016). This data analysis was completed prior to the latest scale upgrades by NOAA (as the WMO Central Calibration Laboratory) to the WMO X2019 scale and by SIO to the SIOX12A scale. Future comparisons within the WMO community should evaluate the implementation of these new scales. Measurements of atmospheric GHGs are reported in units of dry air mole fraction. CO_2 is reported as micromoles CO_2 per mole of dry air ($\mu mol\,mol^{-1}$), abbreviated ppm.

As noted above, Fig. 1a shows the individual co-located atmospheric CO_2 measurement records from air samples collected at Alert (1999–2016). For reference, the average flask pair difference and 1σ (standard deviation) for each individual laboratory can be found in Table S3. Figure 1b shows individual co-located measurement differences (laboratory minus NOAA) along with the darkly shaded WMO-recommended target level of ± 0.1 ppm CO_2. Results from the WMO/IAEA Round Robin experiments spanning this period are indicated by yellow triangles. The annual median values with 95 % CI for each laboratory's difference distribution are shown in Fig. 1c. A summary of these results is listed in Table S9.

The overall (1999–2016) median difference of all available individual measurements from each laboratory relative to NOAA (Table S9) suggests that the CSIRO, MPI-BGC, SIO,

UHEI-IUP, and ECCC CO_2 records from Alert are consistent with the NOAA record to close to the WMO-recommended ± 0.1 ppm CO_2 window at the 95 % CI. However, it is important to be aware that at higher temporal resolution, e.g., yearly, we often observe median differences that exceed the WMO target for one or more consecutive years. As an example, ECCC has a persistent bias of approximately -0.14 ppm from 2001–2007, which is then reduced in 2008. UHEI-IUP meets the WMO-recommended target window from 2005–2008 but has a bias of approximately -0.13 ppm from 2009–2016; the reason for these differences is unclear. An instrument change by SIO in 2012, from an NDIR to a CRDS analyzer, can be seen as a slight reduction of noise in the difference data (Fig. 1b), and the results seem to be slightly more positive after the change, but the results are still within the WMO target. Measurement differences between LSCE and NOAA show that LSCE is consistently high relative to NOAA, resulting in annual differences that exceed the WMO target. However, if we exclude results from the first two comparison years, the LSCE median value offset appears stable at approximately $+0.11$ ppm CO_2. These findings are consistent with annual median results from the same-flask comparison at Alert, where LSCE measurements tend to be greater than ECCC measurements of the same-flask sample (Fig. S1 and Table S10). The overlaid WMO Round Robin results (Fig. 1b, Table S1) show reasonable consistency between the LSCE internal scale and the WMO CO_2 mole fraction scale.

Figure S2 shows median differences (laboratory minus NOAA) by month for each laboratory using data from the entire 17-year period. Overall, with the exception of SIO, we found no obvious evidence of significant seasonal bias in the co-located CO_2 difference distributions. The SIO measurements relative to NOAA during the May–September period relative to the October–March period possibly showed a bias on the order of 0.25 ppm. A similar monthly analysis (not shown here) using results from the SIO and NOAA co-located comparison experiment at Mauna Loa (MLO) did not show a similar seasonal bias result, suggesting that the observed seasonal bias between SIO and NOAA at Alert may be unique to this site. The reason for this is unclear; the sampling at both sites is very similar.

Figure 1d provides the results from similar co-located comparison experiments between CSIRO, SIO, and NOAA at MLO and at CGO, which are plotted with the results from Alert. Table S11 shows that the overall median difference of all individual measurements of CSIRO relative to NOAA is -0.07 (95 % CI: -0.09, -0.04 ppm) at MLO and 0.03 (95 % CI: 0.02, 0.03 ppm) at CGO, respectively, which are relatively consistent with our findings at Alert of -0.05 (95 % CI: -0.06, -0.03) ppm. Also included in the figure are results from co-located comparison experiments between SIO and NOAA at MLO where the overall median difference is -0.11 (95 % CI: -0.13, -0.10) ppm CO_2. This difference is larger than our findings at Alert of -0.02 (95 % CI:
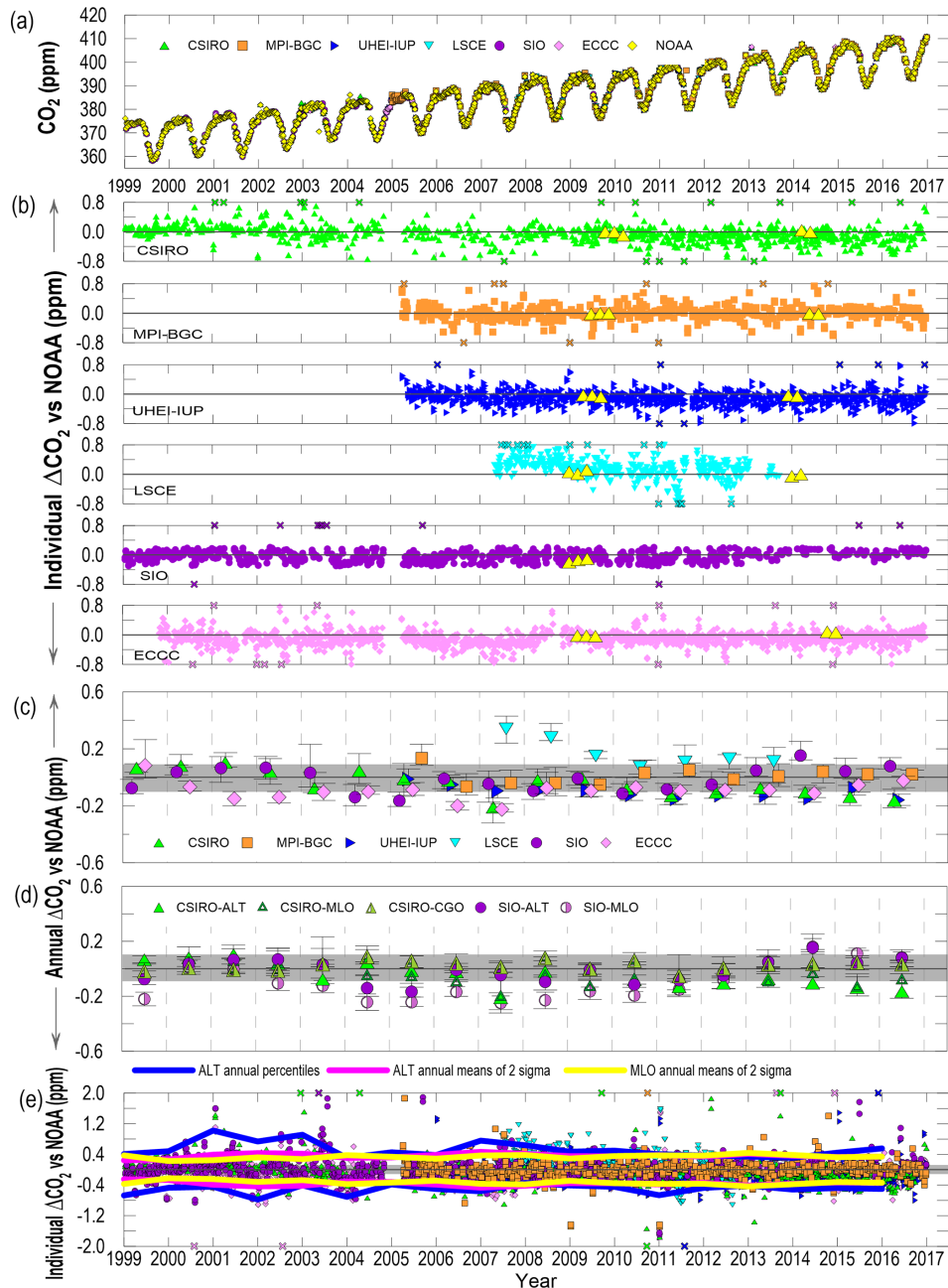
Figure 1. Atmospheric CO_2 comparison results (in ppm) from flask samples taken at Alert, Canada (ALT), Mauna Loa, USA (MLO), and Cape Grim, Australia (CGO) by seven laboratories (CSIRO, MPI-BGC, UHEI-IUP, LSCE, SIO, ECCC, and NOAA). **(a)** Time series of each laboratory's measurements at ALT, showing long-term trends and seasonal patterns in the records. **(b)** Individual ALT CO_2 measurement differences (laboratory minus NOAA) (in ppm). Differences exceeding the y-axis range are plotted with an "X" symbol on the outer axis. Results from the WMO/IAEA Round Robin experiments are overlaid in yellow triangles. The shaded grey band around the zero line indicates the WMO-GAW-recommended measurement agreement goal of ± 0.1 ppm CO_2. **(c)** Annual median CO_2 differences (laboratory minus NOAA) at ALT in ppm, with the lower and upper limits of estimated 95 % confidence intervals (CI). **(d)** Annual median CO_2 differences and 95 % confidence limits (in ppm) of CSIRO minus NOAA at MLO and CGO, and SIO minus NOAA at MLO. Also included are results from ALT in **(c)**. **(e)** Individual measurement differences (laboratory minus NOAA) at ALT (in ppm) for all the laboratories as a collective. Differences exceeding the y-axis range are plotted with an "X" symbol on the outer axis (some extreme outliers have been removed to produce the results). The annual 2.5th and 97.5th percentiles of the entire difference distribution from all laboratories at ALT are shown in blue (from -0.51 to $+0.53$ ppm). The pink lines show the annual means of the $CO_2 \pm 2\sigma$ variations of weekly sampling episodes at ALT (± 0.37 ppm), and the yellow lines show the annual means of the $CO_2 \pm 2\sigma$ variations of weekly sampling episodes at MLO (± 0.34 ppm).

−0.04, −0.01) ppm, but it is still close to the target window of ±0.1 ppm.

Figure 1e shows individual co-located CO_2 measurement differences (in ppm) relative to NOAA for all the laboratories as a collective. Differences exceeding the y-axis range are plotted with an "X" symbol on the appropriate extreme axis. For the approach of using the 2.5th and 97.5th percentiles of the aggregated differenced data (laboratory minus NOAA), an overall collective agreement level of −0.51 to +0.53 ppm ($N = 5691$) was found for the seven laboratories. The corresponding data can be found in Table S12. For the approach of using annual means of the 2σ variation of weekly sampling episodes, an overall measurement agreement is within the ±0.37 ppm window ($N = 923$) also at 95 % of CI. For comparison purposes, we have included the annual means of the combined 2σ variation results at MLO (Fig. 1e and Table S12) shown as the yellow lines (no individual data points are shown) with a comparable result of ±0.34 ppm ($N = 905$).

The observed measurement differences (as annual medians) found in this study can also provide a first estimate of time-dependent uncertainties of observations from a single laboratory. To assess the impacts of those uncertainties on related applications (e.g., long-term trend analysis), we estimate long-term trends of CO_2 from the six individual datasets (CSIRO, MPI-BGC, UHEI-IUP, SIO, ECCC, NOAA) for various 11- and 12-year time periods (2005–2016, 2005–2015, 2006–2016) via Nakazawa's curve-fitting routine (Nakazawa et al., 1997). Table S13 shows very consistent results for these applications. The long-term increases in CO_2 concentrations are 23.62 (2.15 ppm yr^{-1}) ±0.40 ppm (2σ) for 2005–2016, 21.11 ±0.38 ppm (2σ) for 2005–2015, and 20.87 ±0.22 ppm (2σ) for 2006–2016, respectively. The relative differences between the independent datasets are within a narrow range of 1.5 %–2.4 %, indicating that reliable results can be achieved from these individual datasets for long-term trend analysis (> 10 years). It is likely that much larger relative uncertainties would be involved in annual growth rate determination using the corresponding datasets.

3.2 δ^{13}C of CO_2

Stable carbon isotopic ratio measurements in CO_2 are reported commonly as delta values (McKinney et al., 1950; Craig, 1957; Faure, 1986; O'Neil, 1986; Gonfiantini, et al., 1995; Coplen, 1994; Hoefs, 2015; Trolier et al., 1996). A delta value defined here is the relative deviation of two isotopic ratios between a sample and the standard, i.e., the primary VPDB–CO_2 or VPDB scale (VPDB: Vienna Pee Dee Belemnite). As the numerical value of a relative deviation is usually very small (close to 10^{-3}), it is normally multiplied by 10^3 and expressed in per mill (‰) as in the following re-

lationship (Coplen, 1994; Coplen et al., 2002):

$$\delta^{13}C_{\text{samp/VPDB−CO2}} = \left[\left(\left({}^{13}C/{}^{12}C \right)_{\text{sample}} / \left({}^{13}C/{}^{12}C \right)_{\text{VPDB−CO2}} \right) - 1 \right] \times 10^3 ‰.$$

There is no single approach to the realization of the VPDB scale amongst individual laboratories (Table 5); in other words, although the laboratories have created local scales relative to VPDB through a link to NBS19, small inaccuracies in establishing this link may introduce scale differences between the measurement records. This should be kept in mind while interpreting the differences between the data records.

Figure 2a shows the individual co-located atmospheric δ^{13}C–CO_2 measurement records at Alert (1999–2016), and Fig. 2b shows individual co-located measurement differences (laboratory minus INSTAAR) by laboratories. The average overall flask pair difference and 1σ standard deviation for each individual laboratory can be found in Table S4. The overall median difference results (Fig. 2c, Table S14) seem to show that ECCC's δ^{13}C–CO_2 records from Alert agree with INSTAAR to within ±0.01 ‰ at the 95 % CI, although the comparison period was relatively short (1999–2009) and the results change in both directions. Similar to the CO_2 results discussed previously, it is again important to be aware that at higher time resolution, we observe periods where the differences significantly exceed the WMO target and show changes in sign that persist for 1 or more consecutive years. For SIO, we observe a persistent positive offset between SIO and INSTAAR measurements with a median of 0.03 (95 % CI: 0.02, 0.03) ‰, which exists for much of the comparison period. We also observe that while the overall median differences for CSIRO, MPI-BGC, and UHEI-IUP relative to INSTAAR exceed the WMO target window with persistent negative biases ranging from −0.02 to −0.03 (95 % CI: −0.04, −0.02) ‰, the results suggest that the Alert δ^{13}C–CO_2 records from these three laboratories show more agreement with each other than with the INSTAAR reference. It is noted that INSTAAR's measurements are linked to the VPDB–CO_2 scale through the calibrations performed by MPI-BGC (the WMO Central Calibration Laboratory: CCL) via the JRAS-06 realization. The agreement between INSTAAR and MPI-BGC appears to be better after 2015; however, prior to 2015, a bias seems to persist (Fig. 2c). As more laboratories within the community move towards linking their isotopic measurements of air CO_2 to the VPDB–CO_2 scale through the JRAS-06 realization and more comparison results are ultimately expanded over longer time periods and at larger spatial scales, this may improve our ability to assess some of the issues we are currently experiencing. All LSCE annual median values exceed the target window and show that LSCE co-located measurements are consistently more negative relative to INSTAAR with an overall median difference of −0.15 (95 % CI: −0.16, −0.14) ‰

over the available period (2007–2013). LSCE is aware of on-going issues with the traceability of their laboratory scale, which likely accounts for the observed results. Thus, we exclude LSCE measurements from our estimate of the grouped measurement agreement (discussed later). It is also noticed that based on T test results (not shown), the calculated mean differences between laboratories and INSTAAR are statistically significant for almost all of the labs, although they are small; these results indicate that systematic differences do exist, which likely include scale realization differences.

Analysis of the median differences by month for each laboratory relative to INSTAAR (not shown) over the available periods suggests there are no significant seasonal dependencies. We also note that corresponding results from available round robin experiments (Fig. 2b, Table S1) seem generally similar to the individual flask measurement differences from INSTAAR, which provides evidence that analytical procedure, calibration methods, and the approach for realization of the VPDB scale utilized by the participating laboratories may play an important role in the results.

Figure 2d and Table S15 show the similar co-located comparison experiments for $\delta^{13}C$–CO_2 between CSIRO, SIO, and INSTAAR at Mauna Loa (MLO) and between CSIRO and INSTAAR at Cape Grim (CGO). These results are also plotted with the results from Alert. The overall median difference of all individual measurements for $\delta^{13}C$–CO_2 (CSIRO minus INSTAAR) is -0.02 (95 % CI: -0.02, -0.01)‰ at MLO and -0.01 (95 % CI: -0.01, -0.01)‰ at CGO, respectively, which are fairly consistent with the findings at Alert of -0.03 (95 % CI: -0.03, -0.02)‰. The corresponding median difference value of SIO from INSTAAR at MLO is 0.02 (95 % CL: 0.02, 0.02), which is also close to the values of 0.03 (95 % CL: 0.02, 0.03) at Alert.

For an estimation of the overall grouped measurement agreement among the six independent $\delta^{13}C$–CO_2 records at Alert (LSCE has been excluded), the results from two approaches are included in Fig. 2e. The estimated overall measurement agreement (Table S16) among the six independent Alert $\delta^{13}C$–CO_2 records is within the -0.09‰ to $+0.07$‰ window ($n = 3256$). The pink lines in Fig. 2e represent the annual means of 2σ of each weekly $\delta^{13}C$–CO_2 sampling episode. The estimated overall measurement agreement among the six independent Alert $\delta^{13}C$–CO_2 records is within the range of ± 0.06‰ ($n = 899$). For comparison purposes, the annual means of the 2σ values from MLO in Fig. 2e (yellow lines) and Table S16 show comparable results of ± 0.05‰ ($n = 756$).

3.3 $\delta^{18}O$ of CO_2

Oxygen isotopic ratio measurements in CO_2 are also commonly reported as delta values. A delta value is defined as the relative deviation of two isotopic ratios between a sample and the standard (i.e., the primary VPDB–CO_2 scale). Similar to $\delta^{13}C$, the numerical value of the relative deviation in

$\delta^{18}O$ is usually very small and is normally multiplied by 10^3 and expressed in per mill (‰), as in the following relationship:

$$\delta^{18}O_{samp/VPDB-CO2} = \left[\left(\left({}^{18}O/{}^{16}O \right)_{sample} / \left({}^{18}O/{}^{16}O \right)_{VPDB-CO2} \right) - 1 \right] \times 10^3 \text{‰}.$$

The "–CO_2" after VPDB indicates that the scale is linked via the CO_2 from the VPDB carbonate material by a standard procedure of acid digestion using phosphoric acid at 25 °C (McCrea, 1950; O'Neil, 1986; Brand et al., 2009; Wendeberg et al., 2011; Huang et al., 2013). If the local scale used by different laboratories does not follow the same procedure, then $\delta^{18}O$–CO_2 results may not be compatible.

Figure 3a shows the individual co-located atmospheric $\delta^{18}O$–CO_2 measurement records at Alert (1999–2016), and Fig. 3b shows individual co-located measurement differences (laboratory minus INSTAAR) along with the recommended WMO target level of measurement agreement. For reference, the average flask pair difference and 1σ variability for each individual laboratory can be found in Table S5. The overall (1999–2016) median differences of all available individual measurements from each laboratory relative to INSTAAR (Fig. 3c, Table S17) show that the $\delta^{18}O$–CO_2 records by MPI-BGC and ECCC are each roughly compatible with the INSTAAR record to within the WMO-recommended ± 0.05‰ target window, and SIO and CSIRO are just slightly higher than the target at the 95 % CI (by 0.01‰ and 0.03‰, respectively). Similar to CO_2 and $\delta^{13}C$, larger systematic differences are observed in higher temporal-resolution windows and annual median values often exceed the WMO target in opposite directions. For example, for CSIRO's median differences from 1999–2009, the majority of the values fall within the target window. However, a positive bias of approximately 0.16‰ becomes noticeable from 2010 onwards. LSCE measurements tend to be more negative relative to INSTAAR with an overall median value of -0.12 (95 % CI: -0.15, -0.07)‰, and UHEI-IUP measurements tend to be more positive relative to INSTAAR, with an overall value of 0.23 (95 % CI: 0.20, 0.27)‰.

However, the overlaid available results from the periodic round robin experiments (Fig. 3b Table S1) show fewer differences than those in flask samples between INSTAAR and the individual laboratories, including CSIRO, MPI-BGC, UHEI-IUP, and ECCC; this infers that the larger differences observed in flask measurements might be due to variable moisture levels in the samples. Analysis of annual median differences by month for each laboratory relative to INSTAAR (not shown) does not suggest any seasonal dependencies.

Figure 3d and Table S18, respectively, show the results of $\delta^{18}O$–CO_2 from similar co-located comparison experiments between CSIRO and INSTAAR at Mauna Loa (MLO) and at
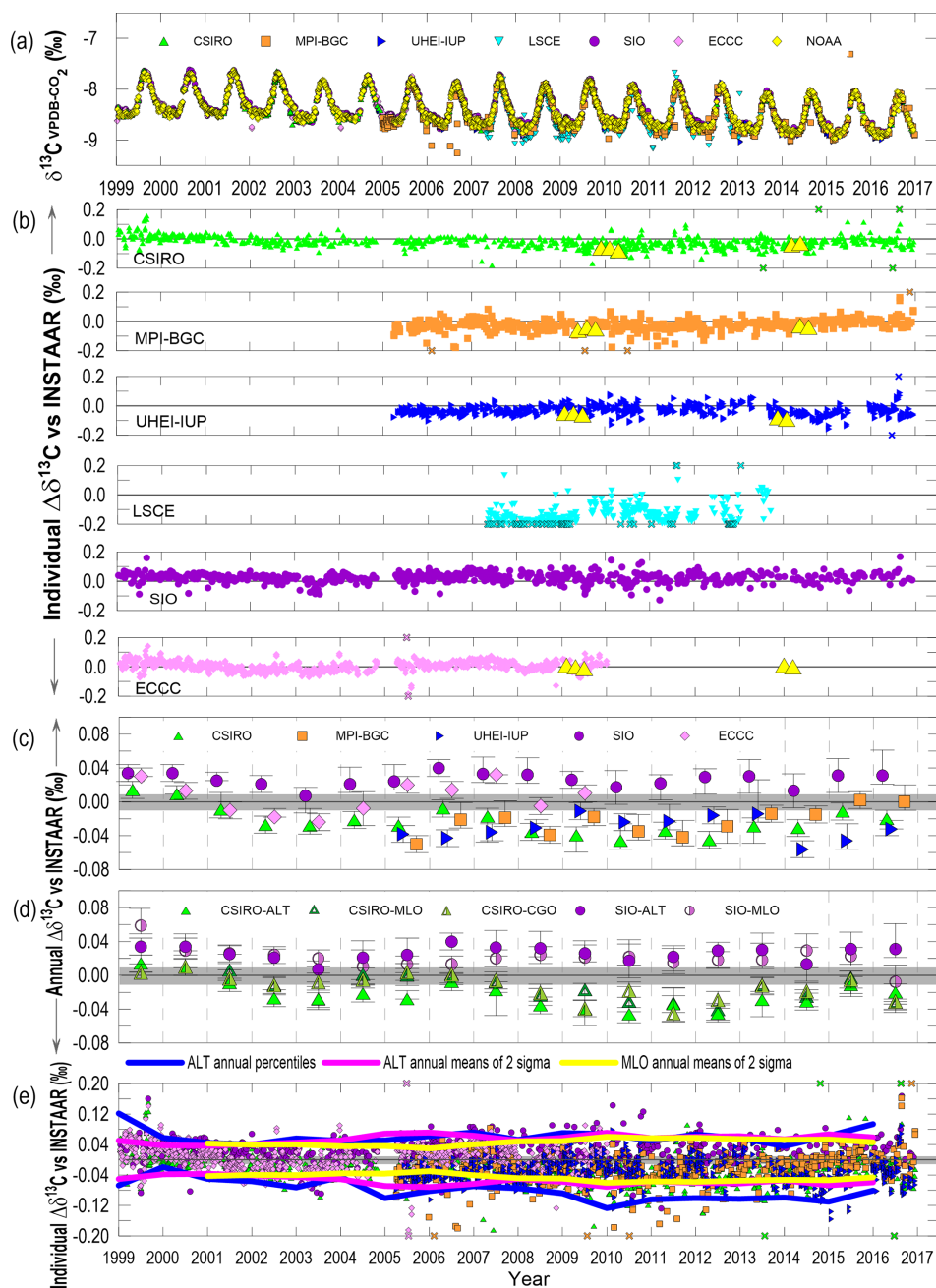
Figure 2. Atmospheric $\delta^{13}C$–CO_2 comparison results, in per mill (‰), from flask samples taken at ALT, MLO, and CGO by seven laboratories. **(a)** Time series of each laboratory's measurements at ALT, showing long-term trends and seasonal patterns in the records. **(b)** Individual ALT $\delta^{13}C$–CO_2 differences (laboratory minus INSTAAR) (in ‰). Differences exceeding the y-axis range are plotted with an "X" symbol on the outer axis. Results from the WMO/IAEA Round Robin experiments are overlaid in yellow triangles. The shaded grey band around the zero line indicates the WMO-GAW-recommended measurement agreement goal of ± 0.01‰. **(c)** Annual median $\delta^{13}C$–CO_2 differences (laboratory minus INSTAAR) at ALT (in ‰), with the lower and upper limits of estimated 95 % CI. **(d)** Annual median $\delta^{13}C$–CO_2 differences and 95 % CI (in ‰), of CSIRO minus INSTAAR at MLO and CGO, and SIO minus INSTAAR at MLO. Also included are results from ALT. **(e)** Individual measurement differences (laboratory minus INSTAAR) at ALT (in ‰) for all the laboratories as a collective. Some extreme outliers have been removed to produce the results. The annual 2.5th and 97.5th percentiles of the entire difference distribution from all laboratories at ALT are shown in blue (-0.09‰ to $+0.07$‰). The pink lines show the annual means of $\pm 2\sigma$ variations of weekly sampling episodes at ALT (± 0.06‰), and the yellow lines show the annual means of $\pm 2\sigma$ variations of weekly sampling episodes at MLO (± 0.05‰).
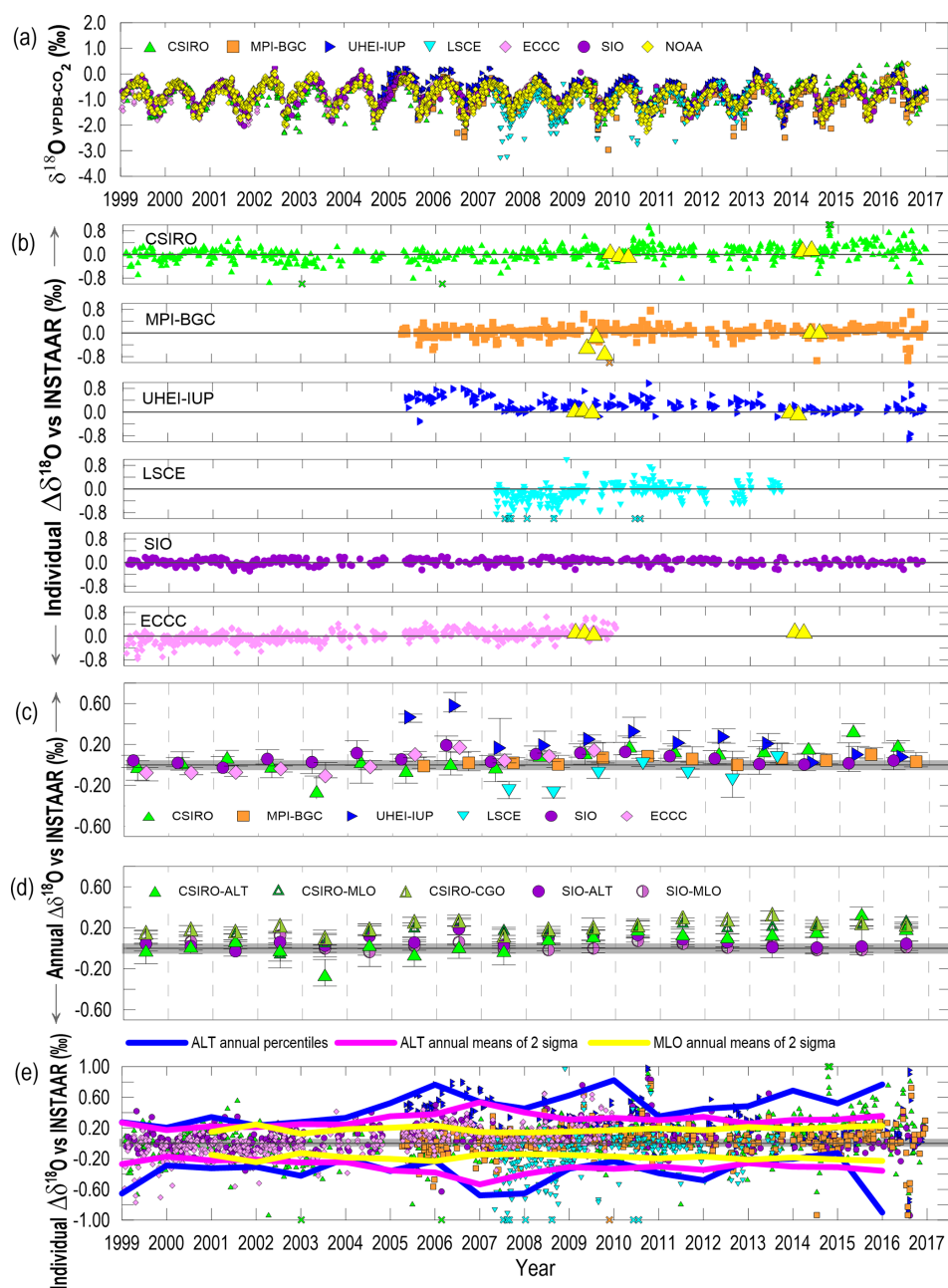
Figure 3. Atmospheric δ^{18}O–CO_2 comparison results, in per mill (‰), from flask samples taken at ALT, MLO, and CGO by seven laboratories. **(a)** Time series of each laboratory's measurements at ALT, showing long-term trends and seasonal patterns in the records. **(b)** Individual ALT δ^{18}O–CO_2 differences (laboratory minus INSTAAR) (in ‰). Differences exceeding the y-axis range are plotted with an "X" symbol on the outer axis. Results from the WMO/IAEA Round Robin experiments are overlaid in yellow triangles. The shaded grey band around the zero line indicates the WMO-GAW-recommended measurement agreement goal of ±0.05 ‰. **(c)** Annual median δ^{18}O–CO_2 differences (laboratory minus INSTAAR) at ALT (in ‰), with the lower and upper limits of estimated 95 % CI. **(d)** Annual median δ^{13}C–CO_2 differences and 95 % CI (in ‰), of CSIRO minus INSTAAR at MLO and CGO, and SIO minus INSTAAR at MLO. Also included are results from ALT. **(e)** Individual differences (laboratory minus INSTAAR) at ALT (in ‰) for all the laboratories as a collective. The annual 2.5th and 97.5th percentiles of the entire difference distribution from all laboratories at ALT are shown in blue (−0.50 ‰ to +0.58 ‰). The pink lines show the annual means of ± 2σ variations of weekly sampling episodes at ALT (± 0.31 ‰), and the yellow lines show the annual means of ± 2σ variations of weekly sampling episodes at MLO (± 0.19 ‰).

Cape Grim (CGO), plotted with the results from Alert. The overall median difference of all individual measurements for CSIRO relative to INSTAAR is 0.18 (95 % CI: 0.17, 0.19) ‰ at MLO and 0.21 (95 % CI: 0.21, 0.22) ‰ at CGO, respectively. While the MLO and CGO results are more or less consistent with each other, they do not align with our overall findings at Alert, which show a value of 0.08 (95 % CI: 0.06, 0.10) ‰. However, as mentioned before, CSIRO's median at ALT from 2010 onwards (0.16 ‰) is fairly similar to the overall value at MLO from 1999 to 2016. Further data may be needed to make any comments on measurement consistency across entire networks for CSIRO and NOAA for $\delta^{18}O$–CO_2. The results between SIO and INSTAAR at Alert and at MLO show a consistent pattern in the difference distribution (SIO relative to INSTAAR) at both sites, with the overall median difference at MLO being 0.03 (95 % CI: 0.02, 0.04) ‰ and the median difference at Alert being 0.06 (95 % CI: 0.05, 0.08) ‰, and thus it is likely that the comparison results at first estimation are representative of measurement consistency across entire networks for SIO and IN-STAAR.

Finally, we estimate a grouped measurement agreement among the seven independent Alert $\delta^{18}O$–CO_2 records by aggregating all individual differences from participating laboratories (relative to INSTAAR) to compute the 2.5th and 97.5th percentiles. This upper and lower limit contains 95 % of the entire difference distribution from all laboratories and represents our best estimate of measurement agreement (blue lines in Fig. 3e). Table S19 shows that the seven independent co-located $\delta^{18}O$–CO_2 records at Alert are compatible to within a −0.50 ‰ to +0.58 ‰ window ($N = 2738$). For the approach of using the means of the 2σ variation from weekly sampling events through the entire period, the corresponding overall measurement agreement is within the range of ± 0.31 ‰ ($n = 872$; pink lines in Fig. 3e). For comparison purposes the annual means of the 2σ values from MLO in Fig. 3e (yellow lines) and Table S19 show a smaller range of ± 0.19 ($n = 729$) ‰.

3.4 CH$_4$

All CH$_4$ measurements are reported relative to the WMO X2004A CH$_4$ mole fraction scale, which is described by Dlugokencky et al. (2005) with updated information (2015) available at https://www.esrl.noaa.gov/gmd/ccl/ch4_scale.html (last access: 17 August 2022). Measurements of atmospheric CH$_4$ are reported in nanomoles (billionths of a mole CH$_4$) per mole of dry air and abbreviated ppb (parts per billion).

Figure 4a shows the individual co-located atmospheric CH$_4$ measurement records at Alert (1999–2016), and Fig. 4b shows individual co-located measurement differences (laboratory minus NOAA) along with the recommended target level of measurement agreement and round robin results. Figure 4c shows the annual median values with 95 % CI for each laboratory's difference distribution. The WMO-GAW-recommended target range is again represented by the dark grey band. Table S20 summarizes these results.

The overall (1999–2016) median difference of all available individual measurements relative to NOAA (Table S20) suggests that the CH$_4$ records of CSIRO, MPI-BGC, UHEI-IUP, and ECCC from Alert agree with NOAA within the WMO-recommended ± 2 ppb CH$_4$ compatibility target window. At higher resolution we sometimes observe differences that exceed the target window for 1 or more consecutive years, without known causes. For example, annual median differences between ECCC and NOAA generally show a consistent offset of approximately −1 ppb except 2003–2004 and 2007, where the offset lies slightly outside the target window. Similar results are observed between LSCE and NOAA where there is a consistent positive offset of ∼ 2 ppb except for 2008 and 2009, where the offset of ∼ 4 ppb lies outside the target window. MPI-BGC and UHEI-IUP show fairly consistent agreement versus NOAA throughout the time period, with just 1 year outside the target window for MPI-BGC in 2012. Annual differences for CSIRO show a slightly negative bias from 1999–2008 with 1 year outside of the target window and a more positive bias from 2009–2016.

Results from the periodic round robin experiments (Fig. 4b, Table S1) are consistent with the co-located comparison results for each individual participating laboratory. Analysis of annual median differences by month for each laboratory relative to NOAA (not shown) does not suggest any seasonal dependencies.

Results from similar co-located comparison experiments between CSIRO and NOAA at Mauna Loa (MLO) and at Cape Grim, (CGO) are plotted with the results from Alert in Fig. 4d. As shown in Table S21, the median difference of all individual CH$_4$ measurements from CSIRO relative to NOAA is 0.66 (95 % CI: 0.38, 0.88) ppb for MLO, 0.11 (95 % CI: −0.07, 0.32) ppb for CGO, and 0.01 (95 % CI: −0.19, 0.21) ppb for Alert, respectively. The results are all within the WMO-recommended compatibility target window. Therefore, the comparison results at the shared site such as Alert could be representative of measurement consistency across entire networks for CSIRO and NOAA for CH$_4$.

Finally, we estimate an overall measurement agreement among the six independent Alert CH$_4$ records of −4.86 to +6.16 ppb ($N = 4472$) over the entire period of 1999–2016 (Table S22), shown in blue lines in Fig. 4e. For the approach of using the means of the 2σ variation from weekly sampling events through the entire period, the estimated overall measurement agreement among the six independent Alert CH$_4$ records is within the range of ± 3.62 ppb ($n = 887$) (pink lines in Fig. 4e). For comparison, we have included the annual means of the combined 2σ variation results of ± 4.88 ppb ($n = 375$) at MLO in yellow lines (Fig. 4e and Table S22).
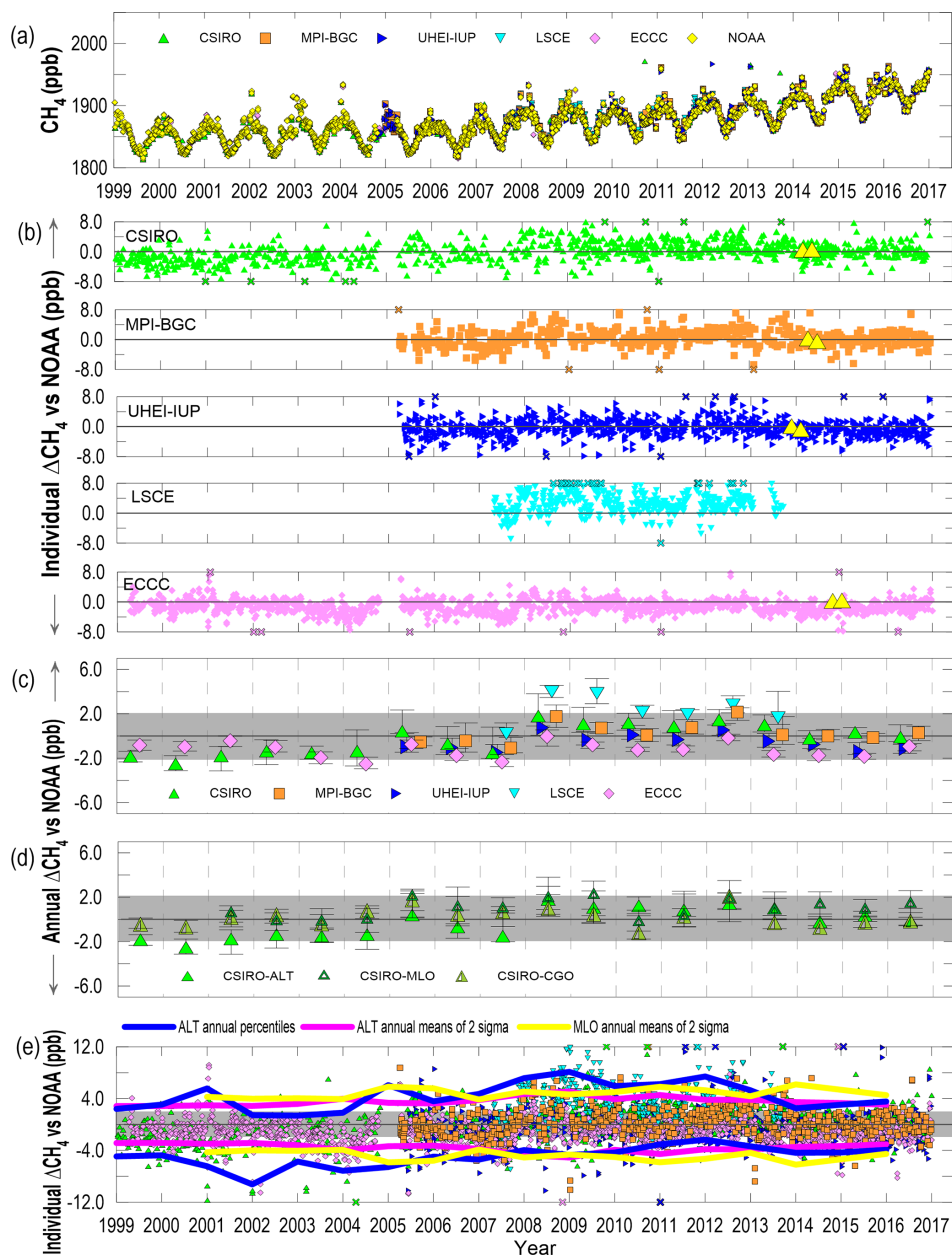
Figure 4. Atmospheric CH_4 comparison results (in ppb) from flask samples taken at ALT, MLO, and CGO by six laboratories (CSIRO, MPI-BGC, UHEI-IUP, LSCE, ECCC, and NOAA). **(a)** Time series of each laboratory's measurements at ALT, showing long-term trends and seasonal patterns in the records. **(b)** Individual CH_4 differences (laboratory minus NOAA) at ALT (in ppb). Differences exceeding the y-axis range are plotted with an "X" symbol on the outer axis. Results from the WMO/IAEA Round Robin experiments are overlaid in yellow triangles. The shaded grey band around the zero line indicates the WMO-GAW-recommended measurement agreement goal of ± 2.0 ppb. **(c)** Annual median CH_4 differences (laboratory minus NOAA) at ALT (in ppb) with the lower and upper limits of estimated 95 % CI. **(d)** Annual median CH_4 differences and 95 % CI (in ppb) of CSIRO minus NOAA at MLO and CGO. Also included are results from ALT. **(e)** Individual differences (laboratory minus NOAA) at ALT (in ppb) for all the laboratories as a collective. Some extreme outliers have been removed to produce the results. The annual 2.5th and 97.5th percentiles of the entire difference distribution from all laboratories at ALT are shown in blue (-4.86 to $+6.16$ ppb). The pink lines show the annual means of $\pm 2\sigma$ variations of weekly sampling episodes at ALT (± 3.62 ppb), and the yellow lines show the annual means of $\pm 2\sigma$ variations of weekly sampling episodes at MLO (± 4.88 ppb).

3.5 N₂O

All N$_2$O measurements are reported relative to the NOAA 2006A N$_2$O mole fraction scale, which is described by Hall et al. (2007) with updated information (2011) available at https://gml.noaa.gov/ccl/n2o_scale.html (last access: 17 November 2023). Measurements of atmospheric N$_2$O are reported as a dry air mole fraction in nanomoles (billionths of a mole N$_2$O) per mole of dry air and abbreviated ppb (parts per billion). All N$_2$O measurements in this study were determined using GC–ECD analytical methodology. These systems typically achieved repeatability of 0.15 to 0.3 ppb, making the comparisons much noisier and, therefore, more difficult to evaluate whether the WMO target goal of ± 0.1 ppb has been achieved. Fortunately, several new spectroscopic methods are now available and capable of providing analytical repeatability of 0.04 to 0.1 ppb (O'Keefe et al., 1999; Griffith et al., 2012). These new methods have a potential to make comparisons less noisy and possibly easier to interpret.

Figure 5a–e and Tables S23–S26 provide the corresponding information for N$_2$O. The seasonal cycle is more clearly defined in the UHEI-IUP dataset (Fig. 5a) than in the other data records due to better precision on their specific GC–ECD. Analytical precision of atmospheric N$_2$O measurement is estimated using agreement between measurements of air collected in two flasks sampled on the same apparatus at the same time. Table S7 summarizes average flask pair agreement based on air samples collected at Alert. Using pair agreement to estimate short-term noise, we find UHEI-IUP and NOAA N$_2$O measurements of flask air with repeatability of 0.13 ± 0.08 ppb and 0.30 ± 0.26 ppb, respectively. The NOAA measurement is less precise because it is derived from a single aliquot of air whereas all other laboratories typically use an average of 2–4 aliquots of sample air. Both NOAA and INSTAAR are limited in the volume of sample that can be used for each of their analyses because of the very large suite of trace gas species measured from the NOAA flask air sample. This has a much more profound impact on estimated N$_2$O precision than for other trace gas species and isotopes.

The overall (1999–2016) median difference of all available individual measurements from each laboratory relative to NOAA (Table S23) shows that the UHEI-IUP and ECCC N$_2$O records from Alert are roughly compatible with the NOAA record to within the WMO-recommended ± 0.1 ppb target window. However, as mentioned in each previous section, at higher resolution, we can observe median differences that well exceed the WMO target for many years. MPI-BGC differences show a consistently positive bias spanning from 2005 to 2014, which is reduced by approximately 2 fold in 2015–2016 when they switched from a Mg(ClO$_4$)$_2$ dryer to a cryocooler. MPI-BGC suggests that these impacts were mostly pronounced during the wetter summer months and attributes the issues to a change in the supplier of the Mg(ClO$_4$)$_2$. A similar problem was reported by Steele et al. (2007). There was no evidence of bias for any of the other

trace species. Differences between LSCE and NOAA, which initially exceed the target by 1.2 ppb, steadily improve each year. By 2013, the final year of the comparison for LSCE, the annual median difference was improved by a factor of ~ 10, to 0.15 ppb but still fell outside the WMO target window. Because the results from the same-flask comparison experiment between LSCE and ECCC (Fig. S3) show a similar difference pattern, this suggests that the sample collection process is not likely the cause of the observed co-located measurement differences. On the other hand, the sameflask air comparison results (Fig. S3, Table S24) for the other laboratories show that the median differences were mostly able to meet the target window, in contrast to the co-located comparisons, suggesting that there may be factors that are specific to the collection of the air itself causing some of the inconsistency among the various laboratories.

Results from the periodic round robin experiments (Fig. 5b, Table S1) are consistent with the co-located comparison results for each participating laboratory. With regard to seasonal dependencies, an analysis of median differences by month (not shown) displayed consistent offsets for each month indicating that the date of sample collection had no bearing on the annual results.

Earlier, we mentioned that analytical precision (estimated from flask pair agreement) of NOAA measurements is about a factor of 2 worse than UHEI-IUP measurements (see Table S7). To explore the impact this may have on our findings, we computed differences relative to the more precise UHEI-IUP N$_2$O record (Fig. S4). As expected, we find the uncertainty in annual median differences relative to the more precise UHEI-IUP N$_2$O record to be considerably smaller than when referenced to NOAA measurements. While the agreement between MPI-BGC and UHEI-IUP measurements improves and the differences of CSIRO and ECCC relative to UHEI-IUP remain more stable over time, our overall findings do not change.

The results from the co-located comparison experiments between CSIRO and NOAA at Mauna Loa (MLO) and at Cape Grim (CGO) (Fig. 5d, Table S25) show the median difference of all individual N$_2$O measurements to be -0.17 (95 % CI: -0.21, -0.13) ppb at MLO, which is consistent with our findings in Alert of -0.17 (95 % CI: -0.20, -0.13) ppb. At CGO this median difference is -0.03 (95 % CI: -0.06, 0.00) ppb, which is slightly smaller than the ALT and MLO results. Considering the previously mentioned effects of water on the N$_2$O measurements, the differences could potentially arise from site-specific sampling parameters, such as CSIRO's change to a cryocooler in 2014 at CGO or NOAA's use of a partially dried sample at CGO (although not at MLO or ALT). However, pinpointing the exact cause is beyond the scope of this paper.

Finally, we estimate a measurement agreement for the six independent Alert N$_2$O data records as a collective, to be within -0.75 to $+1.20$ ppb ($N = 3957$) over the entire period of 1999–2016 (Table S26). For the approach of using
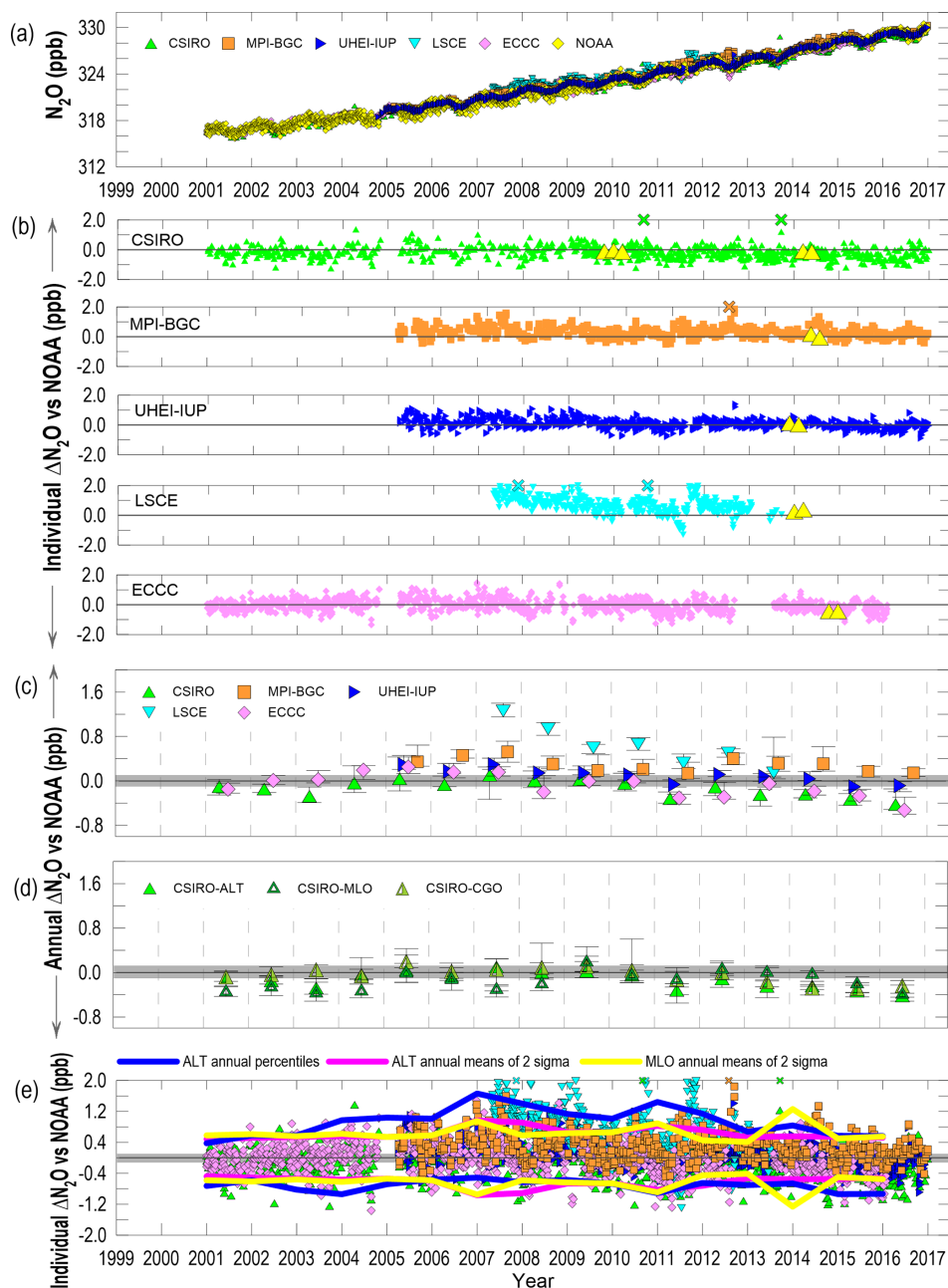
Figure 5. Atmospheric N_2O comparison results (in ppb) from flask samples taken at ALT, MLO, and CGO by six laboratories (CSIRO, MPI-BGC, UHEI-IUP, LSCE, ECCC, and NOAA). **(a)** Time series of each laboratory's measurements at ALT, showing long-term trends and seasonal patterns in the records. **(b)** Individual N_2O differences (laboratory minus NOAA) at ALT (in ppb). Differences exceeding the y-axis range are plotted with an "X" symbol on the outer axis. Results from the WMO/IAEA Round Robin experiments are overlaid in yellow triangles. The shaded grey band around the zero line indicates the WMO-GAW-recommended measurement agreement goal of ± 0.1 ppb. **(c)** Annual median N_2O differences (laboratory minus NOAA) at ALT (in ppb) with the lower and upper limits of estimated 95 % CI. **(d)** Annual median N_2O differences and 95 % CI (in ppb) of CSIRO minus NOAA at MLO and CGO. Also included are results from ALT. **(e)** Individual differences (laboratory minus NOAA) at ALT (in ppb) for all the laboratories as a collective. The annual 2.5th and 97.5th percentiles of the entire difference distribution from all laboratories at ALT are shown in blue (-0.75 to $+1.20$ ppb). The pink lines show the annual means of $\pm 2\sigma$ variations of weekly sampling episodes at ALT (± 0.64 ppb), and the yellow lines show the annual means of $\pm 2\sigma$ variations of weekly sampling episodes at MLO (± 0.64 ppb).
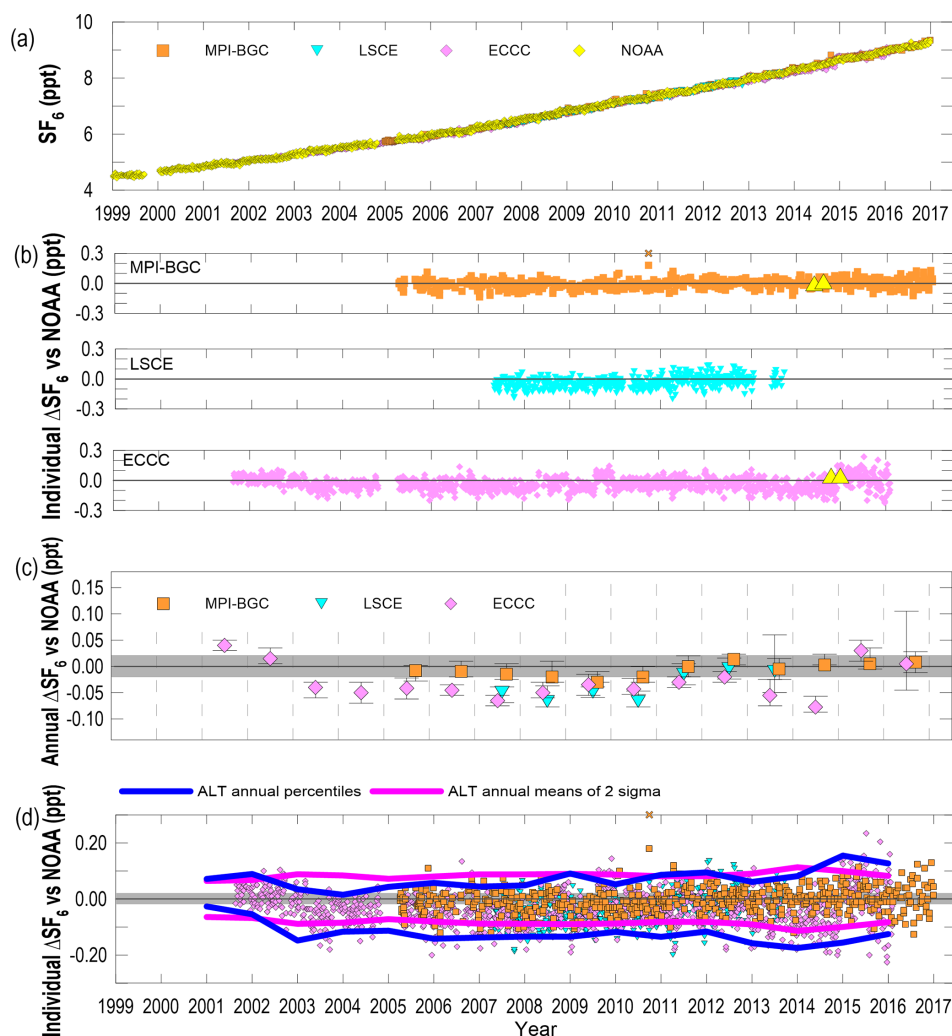
Figure 6. Atmospheric SF$_6$ comparison results (in ppt) from flask samples taken at ALT by four laboratories (MPI-BGC, LSCE, ECCC, and NOAA). **(a)** Time series of each laboratory's measurements at ALT, showing long-term trends and seasonal patterns in the records. **(b)** Individual SF$_6$ differences (laboratory minus NOAA) at ALT (in ppt). Differences exceeding the y-axis range are plotted with an "X" symbol on the outer axis. Results from the WMO/IAEA Round Robin experiments are overlaid in yellow triangles. The shaded grey band around the zero line indicates the WMO-GAW-recommended measurement agreement goal of ± 0.02 ppt. **(c)** Annual median SF$_6$ differences (laboratory minus NOAA) at ALT (in ppt) with the lower and upper limits of estimated 95 % CI. **(d)** Individual differences (laboratory minus NOAA) at ALT (in ppt) for all the laboratories as a collective. The annual 2.5th and 97.5th percentiles of the entire difference distribution from all laboratories at ALT are shown in blue (-0.14 to $+0.09$ ppt). The pink lines show the annual means of $\pm 2\sigma$ variations of weekly sampling episodes at ALT (± 0.09 ppt), and there is no MLO data because neither CSIRO nor SIO measures SF$_6$.

the means of the 2σ variation from weekly sampling events, we estimate a corresponding overall measurement agreement of ± 0.64 ppb ($n = 801$) (pink lines in Fig. 5e). For comparison, we have included the annual means of the combined 2σ variation results of ± 0.64 ppb ($n = 366$) at MLO in yellow lines (Fig. 5e and Table S26).

3.6   SF$_6$

All measurements are reported relative to the NOAA X2014 SF$_6$ mole fraction scale (Hall et al., 2011; Lim et al., 2017). Measurements of atmospheric SF$_6$ are reported in picomoles

(trillionths or 10^{-12} of a mole SF$_6$) per mole of dry air and abbreviated "ppt" (parts per trillion). All SF$_6$ measurements from the four laboratories in this study (MPI-BGC, LSCE, ECCC, and NOAA) were determined using GC-ECD analytical methodology. The estimated repeatability of SF$_6$ measurements, based on replicated injections of standard tank gas, using the dual N$_2$O/SF$_6$ GC-ECD system is ~ 0.04 ppt.

Figure 6a–d and Tables S27–S28 show the corresponding information for SF$_6$. Please note that there is one less figure and table than the other species, because there are no SF$_6$ results from the other sites (MLO and CGO), and

the last figure and table have been shifted up by one, compared to other species. Table S27 and Fig. 6c show that the MPI-BGC and NOAA SF_6 measurements meet the WMO-recommended ± 0.02 ppt SF_6 compatibility window in 11 of the 12 comparison years (2005–2016). Annual median differences between ECCC and NOAA measurements for 2003–2014 show a constant median offset of -0.05 ppt. The annual differences between LSCE and NOAA measurements for 2007 to 2010 show a similar average offset of approximately -0.05 ppt but showed good agreement from 2011 to 2013. Results from the periodic round robin experiments (Fig. 6b, Table S1) are consistent with the co-located comparison results for each participating laboratory. Again, we find the analysis of median differences by month for each laboratory (not shown) does not indicate any seasonal dependencies.

We find the four independent co-located SF_6 records at Alert (Table S28) are consistent to within a window of -0.14 to $+0.09$ ppt ($N = 2359$) using 2.5th and 97.5th percentiles and ± 0.09 ppt ($N = 723$) using the mean of the 2σ approach over the time period, respectively. Figure 6d shows individual measurement differences relative to the NOAA reference for all laboratories, the WMO-recommended target range (dark grey band), and our estimate of the overall measurement agreements (in blue and pink lines). There are no SF_6 measurements at MLO or CGO to make general comparisons with the Alert data records.

4　Summary and conclusions

We presented a comparison of measurements of CO_2, CH_4, N_2O, and SF_6 and the stable isotope ratios of CO_2 ($\delta^{13}C$, $\delta^{18}O$) in co-located air samples collected at Alert, Nunavut, Canada, by seven laboratories (ECCC, CSIRO, MPI-BGC, UHEI-IUP, LSCE, SIO, and NOAA (in collaboration with INSTAAR)) spanning 17 years. We also evaluated the consistency of measurements between certain laboratories (CSIRO, SIO, and NOAA/INSTAAR) at three sites (ALT, MLO, and CGO), where other co-located flask sampling programs operate.

From this work, we find that the co-located atmospheric CO_2 and CH_4 measurement records from Alert by CSIRO, MPI-BGC, SIO, UHEI-IUP, ECCC, and NOAA are compatible to the WMO network compatibility goals within ± 0.1 ppm CO_2 and ± 2 ppb CH_4 at the 95 % CI, respectively, over the 17-year period. In addition, we find that the co-located comparison programs at MLO and CGO show similar agreement levels to those at Alert within a range of ± 0.1 ppm for CO_2 between CSIRO, SIO, and NOAA records and within a range of ± 2 ppb for CH_4 between CSIRO and NOAA records. An important caveat to these CO_2 and CH_4 results is that we often observe periods where the biases between datasets exceed the WMO target levels and may persist as a systematic bias for months or years,

which could impact our observed compatibility. Our analysis shows that for $\delta^{13}C$–CO_2, $\delta^{18}O$–CO_2, N_2O, and SF_6, our estimate of the overall measurement agreements during the time of this study exceeds the WMO-recommended targets. Differences in the respective local-scale implementations for the isotopes of CO_2, possible moisture effects for $\delta^{18}O$–CO_2, and the analytical precision of the instruments used for N_2O and SF_6 are possible limiting factors for these results. In addition, the N_2O may have some biases introduced by sample collection procedures.

Further analysis shows that the overall results observed for CSIRO, SIO, and NOAA/INSTAAR's CO_2, CH_4, and $\delta^{13}C$–CO_2 for the study period are roughly consistent among the three sites (ALT, MLO, and CGO), implying that merging these records could be done across these specific networks. However, for the $\delta^{18}O$–CO_2 and N_2O records, future data may be needed to make definitive statements about compatibility across networks.

Although most of the co-located independent CO_2 and CH_4 atmospheric records at Alert meet the WMO-recommended targets when considering the results over the entire study period (1999–2016), meeting the compatibility targets for other trace gas species and stable isotopes in CO_2 continues to be a challenge. The independent measurement records could still be used together for various scientific applications (e.g., long-term trend analysis of CO_2 in Sect. 3.1), even though individual data points are not fully compatible with the WMO-GAW-recommended targets. Furthermore, if we provide data users with the estimated overall measurement agreements for multiple records, they could then take these estimates into account, along with the measurement uncertainties from individual records, while using the datasets for relevant applications.

For each trace gas species and isotope, we have estimated an overall measurement agreement among the Alert records by aggregating all individual differences from each participating laboratory (relative to the NOAA or INSTAAR reference) and then computing the 2.5th and 97.5th percentiles for the entire available periods. This upper and lower limit contains 95 % of the entire difference distribution from all participating laboratories and represents our best estimate of measurement agreement for these data records. The ranges of the estimated overall measurement agreement when combining all individual flask records from Alert over the entire available periods are -0.51 to $+0.53$ ppm for CO_2, -0.09‰ to $+0.07$‰ for $\delta^{13}C$–CO_2, -0.50‰ to $+0.58$‰ for $\delta^{18}O$–CO_2, -4.86 to $+6.16$ ppb for CH_4, -0.75 to $+1.20$ ppb for N_2O, and -0.14 to $+0.09$ ppt for SF_6. Using another alternative approach as discussed in Sect. 2.6., we provide the means of the 2σ of each weekly sampling episode, involving all participating laboratories over the entire available time period, which are ± 0.37 ppm for CO_2, ± 0.06‰ for $\delta^{13}C$–CO_2, ± 0.31‰ for $\delta^{18}O$–CO_2, ± 3.62 ppb for CH_4, ± 0.64 ppb for N_2O, and ± 0.09 ppt for SF_6. Results from this analysis reveal overall cumulative differences due to errors introduced

at one or more steps in the entire atmospheric measurement process, including sampling and analytical procedures.

In summary, this study assesses the level of measurement agreement among individual programs by comparing co-located flask air measurements. It enhances confidence in the uncertainty estimation while using those datasets either individually or collectively across diverse applications. Conducting such comprehensive analysis regularly is advisable to detect potential issues and monitor any scale and/or instrumentation changes. It is recommended that future analyses be carried out every 2 years by a dedicated entity and be reported regularly during WMO/IAEA GGMT meetings.

References

Allison, C. E. and Francey, R. J.: Verifying Southern Hemisphere trends in atmospheric carbon dioxide stable isotopes, J. Geophys. Res., 112, D21304, https://doi.org/10.1029/2006JD007345, 2007.

Allison, C. E., Francey, R. J., and Meijer, H. A. J.: Recommendations for the Reporting of Stable Isotope Measurements of Carbon and Oxygen in CO_2 Gas, in: Reference and Intercomparison Materials for Stable Isotopes of Light Elements, 155 p., https://inis.iaea.org/collection/NCLCollectionStore/_Public/27/021/27021327.pdf?r=1 (last access: 30 November 2023), 1995.

Bollenbacher, A. F., Guenther, P. R., Keeling, C. D., Stewart, E. F., Wahlen, M., and Whorf, T. P.: Calibration Methodology for the Scripps $^{13}C/^{12}C$ and $^{18}O/^{16}O$ Stable Isotope Program 1992–1996. A Report Prepared for the Global Environmental Monitoring Program of the World Meteorological Organization, 156 pp., bollenbacher_calibration_methodology_isotope_program_2000.pdf, https://scrippsco2.ucsd.edu/assets/publications/bollenbacher_calibration_methodology_isotope_program_2000.pdf, last access: 7 December 2023)), 2000.

Brand, W. A., Huang, L., Mukai, H., Chivulescu, A., Richter, J. M., and Rothe, M.: How well do we know VPDB? Variability of $\delta^{13}C$ and $\delta^{18}O$ in CO_2 generated from NBS19-calcite, Rapid Commun. Mass Spectrom., 23, 915–926, 2009.

Brand, W. A., Assonov, S. S., and Coplen, T. B.: Correction for the ^{17}O interference in δ (^{13}C) measurements when analyzing CO_2 with stable isotope mass spectrometry (IUPAC Technical Report), Pure Appl. Chem., 82, 1719–1733, https://doi.org/10.1351/PAC-REP-09-01-05, 2010.

Bousquet, B., Peylin, P., Ciais, P., Le Quéré, C., Friedlingstein, P. and Tans, P. P.: Regional Changes in Carbon Dioxide Fluxes of Land and Oceans Since 1980, Science, 290, 1342–1346, 2000.

Campbell, M. J. and Gardner, M. J.: Calculating confidence intervals for some non-parametric analyses, British Medical Journal (Clinical Research Edition), 296, 1454–1456, 1988.

Chevallier, F. Ciais, P., Conway, T. J., Aalto, T., Anderson, B. E., Bousquet, P., Brunke, E. G., Ciattaglia, L., Esaki, Y., Fröhlich, M., Gomez, A., Gomez-Pelaez, A. J., Haszpra, L., Krummel, P. B., Langenfelds, R. L., Leuenberger, M., Machida, T., Maignan, F., Matsueda, H., Morguí, J. A., Mukai, H., Nakazawa, T., Peylin, P., Ramonet, M., Rivier, L., Sawa, Y., Schmidt, M., Steele, L. P., Vay, S. A., Vermeulen, A. T., Wofsy, S., and Worthy, D.: CO_2 surface fluxes at grid point scale estimated from a global 21-year

reanalysis of atmospheric measurements, J. Geophys. Res., 115, D21307, https://doi.org/10.1029/2010JD013887, 2010.

Conway, T. J., Tans, P. P., Waterman, L. S., Thoning, K. W., Kitzis, D., Masarie, K. A., and Zhang, N.: Evidence for interannual variability of the carbon cycle from the National Oceanic and Atmospheric Administration/Climate Monitoring and Diagnostics Laboratory Global Air Sampling Network, J. Geophys. Res.-Atmos., 99, 22831–22855, https://doi.org/10.1029/94JD01951, 1994.

Coplen, T.: Reporting of stable hydrogen, carbon and oxygen isotopic abundances, IUPAC, 66, 273–276, 1994.

Coplen, T. B., Hopple, J. A., Bohlke, J. K., Peiser, H. S., Rieder, S. E., Krouse, H. R., Rosman, K. J. R., Ding, T., Vocke, Jr., R. D., Revesz, K. M., Lamberty, A., Taylor, P., and De Bievre, P.: Compilation of minimum and maximum isotope ratios of selected elements in naturally occurring terrestrial materials and reagents, U.S. G.S. Water-Resources Investigations Report 01-4222, Reston, Virginia, https://doi.org/10.3133/wri014222, 2002.

Craig, H.: Isotopic standards for carbon and oxygen and correction factors for mass-spectrometric analysis of carbon dioxide, Geochim. Cosmochim. Acta, 12, 133–149, 1957.

Dlugokencky, E. J., Steele, L. P., Lang, P. M., and Masarie, K. A.: The growth rate and distribution of atmospheric methane, J. Geophys. Res., 99, 17, https://doi.org/10.1029/94JD01245, 1994.

Dlugokencky, E. J., Myers, R. C., Lang, P. M., Masarie, K. A., Crotwell, A. M., Thoning, K. W., Hall, B. D., Elkins, J. W., and Steele, L. P.: Conversion of NOAA atmospheric dry air CH_4 mole fractions to a gravimetrically prepared standard scale, J. Geophys. Res., 110, D18306, https://doi.org/10.1029/2005JD006035, 2005.

Fan, S., Gloor, M., Mahlman, J., Pacala, S., Sarmiento, J., Takahashi, T. and Tans, P.: A large terrestrial carbon sink in North America implied by atmospheric and oceanic CO_2 data and models, Science, 282, 442–446, 1998.

Faure, G.: 26 Carbon, In: Principles of Isotope Geology (second edition). John Wiley & Sons, New York, p. 491, https://www.osti.gov/biblio/5648561 (last access: 4 December 2023), 1986.

Francey, R. J., Steele, L. P., Spencer, D. A., Langenfelds, R. L., Law, R. M., Krummel, P. B., Fraser, P. J., Etheridge, D. M., Derek, N., Coram, S. A., Cooper, L. N., Allison, C. E., Porter, L., and Baly, S.: The CSIRO (Australia) measurement of greenhouse gases in the global atmosphere, in: Report of the 11th WMO/IAEA Meeting of Experts on Carbon Dioxide Concentration and Related Tracer Measurement Techniques, Tokyo, Japan, September 2001, WMO-GAW Report- 1138, edited by: Toru, S. and Kazuto, S., 97–111 pp., https://library.wmo.int/idurl/4/41199 (last access: 28 November 2023) 2003.

Friedlingstein, P., Jones, M. W., O'Sullivan, M., Andrew, R. M., Bakker, D. C. E., Hauck, J., Le Quéré, C., Peters, G. P., Peters, W., Pongratz, J., Sitch, S., Canadell, J. G., Ciais, P., Jackson, R. B., Alin, S. R., Anthoni, P., Bates, N. R., Becker, M., Bellouin, N., Bopp, L., Chau, T. T. T., Chevallier, F., Chini, L. P., Cronin, M., Currie, K. I., Decharme, B., Djeutchouang, L. M., Dou, X., Evans, W., Feely, R. A., Feng, L., Gasser, T., Gilfillan, D., Gkritzalis, T., Grassi, G., Gregor, L., Gruber, N., Gürses, Ö., Harris, I., Houghton, R. A., Hurtt, G. C., Iida, Y., Ilyina, T., Luijkx, I. T., Jain, A., Jones, S. D., Kato, E., Kennedy, D., Klein Goldewijk, K., Knauer, J., Korsbakken, J. I., Körtzinger, A., Landschützer, P., Lauvset, S. K., Lefèvre, N., Lienert, S.,

Liu, J., Marland, G., McGuire, P. C., Melton, J. R., Munro, D. R., Nabel, J. E. M. S., Nakaoka, S.-I., Niwa, Y., Ono, T., Pierrot, D., Poulter, B., Rehder, G., Resplandy, L., Robertson, E., Rödenbeck, C., Rosan, T. M., Schwinger, J., Schwingshackl, C., Séférian, R., Sutton, A. J., Sweeney, C., Tanhua, T., Tans, P. P., Tian, H., Tilbrook, B., Tubiello, F., van der Werf, G. R., Vuichard, N., Wada, C., Wanninkhof, R., Watson, A. J., Willis, D., Wiltshire, A. J., Yuan, W., Yue, C., Yue, X., Zaehle, S., and Zeng, J.: Global Carbon Budget 2021, Earth Syst. Sci. Data, 14, 1917–2005, https://doi.org/10.5194/essd-14-1917-2022, 2022.

GAW Report #168: 13th WMO/IAEA Meeting of Experts on Carbon Dioxide Concentration and Related Tracers Measurement Techniques, Boulder, Colorado, USA, 19–22 September, 2005, edited by: Miller, J. B., https://library.wmo.int/idurl/4/47435 (last access: 17 November 2023), 2006.

GAW Report #194: 15th WMO/IAEA Meeting on Carbon Dioxide, Other Greenhouse Gases and Related Tracer Measurement Techniques, Jena, Germany, 7–10 September 2009, edited by: Brand, W. A., https://library.wmo.int/idurl/4/58718 (last access: 17 November 2023), 2011.

GAW Report #229: 18th WMO/IAEA Meeting on Carbon Dioxide, Other Greenhouse Gases and Related Tracer Measurement Techniques, (GGMT-2015), La Jolla, CA, USA, 13–17 September 2015, edited by: Tans, Pieter and Zellweger, C., https://library.wmo.int/idurl/4/55285 (last access: 17 November 2023), 2016.

GAW Report #242: 19th WMO/IAEA meeting on Carbon Dioxide, Other Greenhouse Gases and Related Measurement Techniques (GGMT-2017), Dubendorf, Switzerland, 27–31 August 2017, edited by: Crotwell, A. and Steinbach, M., https://library.wmo.int/idurl/4/37000 (last access: 17 November 2023), 2018.

GAW Report #255: 20th WMO/IAEA Meeting on Carbon Dioxide, Other Greenhouse Gases and Related Measurement Techniques (GGMT-2019), Jeju Island, South Korea, 2–5 September 2019, edited by: Crotwell, A., Lee, H., and Steinbach, M., https://library.wmo.int/idurl/4/57135 (last access: 17 November 2023), 2020.

Ghosh, P. and Brand, W. A.: The effect of N_2O on the isotopic composition of air-CO_2 samples, Rapid Commun. MS., 18, 1830–1838, https://doi.org/10.1002/rcm.1560, 2004.

Gloor, M., Fan, S.-M., Pacala, S., and Sarmiento, J.: Optimal sampling of the atmosphere for purpose of inverse modeling: A model study, Global Biogeochem. Cy., 14, 407–428, https://doi.org/10.1029/1999GB900052, 2000.

Gonfiantini, R., Stichiler, W., and Rozanski, K.: Standards and Intercomparison materials distributed by International Atomic Energy Agency for stable isotope measurements, in: IAEA-TECDOC-825, References and Intercomparison materials for stable isotopes of light elements, 13–29, https://inis.iaea.org/collection/NCLCollectionStore/_Public/27/021/27021327.pdf?r=1 (last access: 4 December 2023), 1995.

Griffith, D. W. T., Deutscher, N. M., Caldow, C., Kettlewell, G., Riggenbach, M., and Hammer, S.: A Fourier transform infrared trace gas and isotope analyser for atmospheric applications, Atmos. Meas. Tech., 5, 2481–2498, https://doi.org/10.5194/amt-5-2481-2012, 2012.

Guenther, P. R., Bollenbacher, A. F., Keeling, C. D., Stewart, E. F., and Wahlen, M.: Calibration Methodology for the Scripps $^{13}C/^{12}C$ and $^{18}O/^{16}O$ Stable Isotope Program 1996–2000, A Report Prepared for the Global Environmental Monitoring

Program of the World Meteorological Organization, 123 pp., guenther_calibration_methodology_isotope_program_2001.pdf, https://scrippsco2.ucsd.edu/assets/publications/guenther_ calibration_methodology_isotope_program_2001.pdf (last access: 17 November 2023), 2001.

Gurney, K. R., Law, R. M., Denning, A. S., Rayner, P. J., Baker, D., Bousquet, P., Bruhwiler, L. M. P., Chen, Y.-H., Ciais, P., Fan, S., Fung, I. Y., Gloor, M., Heimann, M., Higuchi, K., John, J., Maki, T., Maksyutov, S., Masarie, K. A., Peylin, P., Prather, M., Pak, B. C., Rangerson, J., Sarmiento, J., Taguchi, S., Takahashi, T., and Yuen, C.-W.: Towards robust regional estimates of CO_2 sources and sinks using atmospheric transport models, Nature, 415, 626–630, https://doi.org/10.1038/415626a, 2002.

Hall, B. D., Dutton, G. S., and Elkins, J. W.: The NOAA nitrous oxide standard scale for atmospheric observations, J. Geophys. Res., 112, D09305, https://doi.org/10.1029/2006JD007954, 2007.

Hall, B. D., Dutton, G. S., Mondeel, D. J., Nance, J. D., Rigby, M., Butler, J. H., Moore, F. L., Hurst, D. F., and Elkins, J. W.: Improving measurements of SF_6 for the study of atmospheric transport and emissions, Atmos. Meas. Tech., 4, 2441–2451, https://doi.org/10.5194/amt-4-2441-2011, 2011.

Heimann, M. and Keeling, C. D.: A three-dimensional model of atmospheric CO_2 transport based on observed winds: 2, Model description and simulated tracer experiments in Aspects of Climate Variability in the Pacific and Western Americas, Geophysical Monograph Series 55, edited by: Peterson, D. H., American Geophysical Union, Washington DC, 237–275, https://doi.org/10.1029/GM055p0237, 1989.

Heimann, M., Jordan, A., Brand, W. A., Lavric, J. V., Moossen, H., and Rothe, M.: The atmospheric flask sampling program of MPI-BGC, https://doi.org/10.17617/3.8r, 2022.

Houweling, S., Bergamaschi, P., Chevallier, F., Heimann, M., Kaminski, T., Krol, M., Michalak, A. M., and Patra, P.: Global inverse modeling of CH_4 sources and sinks: an overview of methods, Atmos. Chem. Phys., 17, 235–256, https://doi.org/10.5194/acp-17-235-2017, 2017.

Hoefs, J.: 1.3.1.2. The Delta Value, In: Stable Isotope Geochemistry", Springer, Berlin, p. 8, http://ndl.ethernet.edu.et/bitstream/ 123456789/71312/1/2015_Book_StableIsotopeGeochemistry. pdf (last access: 7 December 2023), 2015.

Huang, L., Chivulescu, A., Ernst, D., Zhang, W., Norman, A.-L., and Lee, Y.-S.: Maintaining consistent traceability in high-precision isotope measurements of CO_2: a way to verify atmospheric trends of $\delta^{13}C$ and $\delta^{18}O$, Atmos. Meas. Tech., 6, 1685–1705, https://doi.org/10.5194/amt-6-1685-2013, 2013.

Keeling, C. D.: The Concentration and Isotopic Abundances of Carbon Dioxide in the Atmosphere, Tellus, 12, 200–203, 1960.

Keeling, R. F., Guenther, P. R., Walker, S., and Moss, D. J.: Scripps reference gas calibration system for carbon dioxide-in-nitrogen and carbon dioxide-in-air standards: revision of 2012, Scripps Institution of Oceanography, Microsoft Word – Mano_Report7rev32 – typos fixed.doc (https: //scrippsco2.ucsd.edu/assets/publications/manometry_report_ scripps_ref_gas_calibration_revision_of_2012_pub_2016.p, last access: 17 November 2023), 2016.

Langenfeld, R. L., Krummel, P. B., Allison, C. E., Francey, R. J., Steele, L.P., and Cooper, L. N. (CSIRO), Worthy, D. E. J., Huang, L., Ernst, D., and Chivulescu, A. (MSC): Intercomparison of MSC And CSIRO trace gas from Alert and Estevan point, in: Canadian Baseline Program, Summary of Progress to 2002, 67–76, 2003.

Langenfelds, R. L., Guerette E-A., Steele L. P., Krummel P. B., Spencer D. A., Loh Z. M., Gregory R. L., Thornton D. P., Howden R. T., and Fraser P. J.: Atmospheric methane, carbon dioxide, carbon monoxide, hydrogen and nitrous oxide from Cape Grim flask samples analysed by gas chromatography, in Baseline Atmospheric Program (Australia), 2014–2016, edited by: Langenfelds, R., Derek, N., and Cleland, S. L., Bureau of Meteorology and CSIRO Environment, Melbourne, Australia, in press, 2023.

Levin, I., Karstens, U., Eritt, M., Maier, F., Arnold, S., Rzesanke, D., Hammer, S., Ramonet, M., Vítková, G., Conil, S., Heliasz, M., Kubistin, D., and Lindauer, M.: A dedicated flask sampling strategy developed for Integrated Carbon Observation System (ICOS) stations based on CO_2 and CO measurements and Stochastic Time-Inverted Lagrangian Transport (STILT) footprint modelling, Atmos. Chem. Phys., 20, 11161–11180, https://doi.org/10.5194/acp-20-11161-2020, 2020.

Lim, J. S., Lee, J., Moon, D., Kim, J. S., Lee, J. D. and Hall, B. D.: Gravimetric standard gas mixtures for global monitoring of atmospheric SF_6, Anal. Chem., 89, 12068–12075, https://doi.org/10.1021/acs.analchem.7b02545, 2017.

Lueker, T., Keeling, R., Bollenbacher, A. F., Walker, S. J., Morgan, E., and Brooks, M.: Calibration Methodology for the Scripps $^{13}C/^{12}C$ and $^{18}O/^{16}O$ stable isotope program 1992–2018, Scripps Institution of Oceanography Technical Report, 1–39, https://escholarship.org/uc/item/4n93p288 (last access: last access: 17 November 2023) 2020.

Masarie, K. A. and Tans, P. P.: Extension and integration of atmospheric carbon dioxide data into a globally consistent measurement record, J. Geophys. Res.-Atmos., 100, 11593–11610, 1995.

Masarie, K. A., Langenfelds, R. L., Allison, C. E., Conway, T. J., Dlugokencky, E. J., Francey, R. J., Novelli, P. C., Steele, L. P., Tans, P. P., Vaughn, B., and White, J. W. C.: NOAA/CSIRO Flask Air Intercomparison Experiment: A strategy for directly assessing consistency among atmospheric measurements made by independent laboratories, J. Geophys. Res., 106, 20445–20464, 2001.

Masarie, K. A., Conway, T., Dlugokencky, E. J., Novelli, P., Tans, P., (NOAA), Worthy, D., and Ernst, M. (MSC): The MSC/NOAA ongoing flask air intercomparison experiment, In: Canadian Baseline Program, Summary of Progress to 2002, 64–66, 2003.

Masarie, K. A., Peters, W., Jacobson, A. R., and Tans, P. P.: ObsPack: a framework for the preparation, delivery, and attribution of atmospheric greenhouse gas measurements, Earth Syst. Sci. Data, 6, 375–384, https://doi.org/10.5194/essd-6-375-2014, 2014.

McCrea, J. M.: On the isotopic chemistry of carbonates and a paleo temperature scale, J. Chem. Phys., 18, 849–857, 1950.

McKinney, C. R., McCrea, J. M., Epstein, S., Allen, H. A., and Urey, H. C.: Improvements in Mass Spectrometers for the Measurement of Small Differences in isotope Abundance Ratios, The Review of Scientific Instruments, Vol. 21, No. 8, 724–730, https://doi.org/10.1063/1.1745698, 1950.

Michel, S.: The revised INSTAAR data set for $^{13}C-CO_2$: How do we measure up to other stable isotope laboratories, and how can we work together to make the most of our data?, The 21st Expert Meeting on Greenhouse Gas Measurement Techniques (WMO

GAW GGMT-2022), Wageningen, Netherlands, 19–21 September, 2022, 85 pp., https://www.ggmt2022.online/wp-content/uploads/ggmt2022/posters/85_GGMT_Sylvia_Michel.pdf (last access: 7 December 2023), 2022.

Mook, W. G. and Jongsma, J.: Measurement of the N_2O correction for $^{13}C/^{12}C$ ratios of atmospheric CO_2 by removal of N_2O, Tellus B, 398, https://doi.org/10.1111/j.1600-0889.1987.tb00274.x, 1987.

Nakazawa, T., Ishizawa, M., Higuchi, K., and Trivett, N.B.: Two curve fitting methods applied to CO_2 flask data, Environmetrics, 8, 197–218, https://www.researchgate.net/publication/229927127_Two_curve_fitting_method_applied_to_CO2_flask_data (last access: 4 December 2023), 1997.

Neubert, R.: Messung der stabilen Isotopomere des atmosphärischen Kohlendioxids, PhD, Institut für Umweltphysik, Heidelberg University, Germany, 1998.

O'Keefe, A., Scherer, J. J., and Paul, J. B.: Integrated cavity output spectroscopy, Chem. Phys. Lett., 307, 343–349, https://doi.org/10.1016/S0009-2614(99)00547-3, 1999.

O'Neil, J. R.: "Appendix: Terminology and Standards", in: Valley, J. W., Taylor, H. P., and O'Neil, J. R., "Stable Isotopes in high temperature geological processes", 561–570, http://www.minsocam.org/msa/rim/rim16.html (last access: 4 December 2023), 1986.

Peters, W., Jacobson, A. R., Sweeney, C., Andrews, A., Conway, T. J., Masarie, K. A., Miller, J. B., Bruhwiler, L., Pétron, G., Hirsch, A., Worthy, D., van der Werf, G., Randerson, J. T., Wennberg, P., Krol, M., and Tans, P. P.: An atmospheric perspective on North American carbon dioxide exchange: CarbonTracker, P. Natl. Acad. Sci. USA, 104, 18925–18930, https://doi.org/10.1073/pnas.0708986104, 2007.

Peylin, P., Law, R. M., Gurney, K. R., Chevallier, F., Jacobson, A. R., Maki, T., Niwa, Y., Patra, P. K., Peters, W., Rayner, P. J., Rödenbeck, C., van der Laan-Luijkx, I. T., and Zhang, X.: Global atmospheric carbon budget: results from an ensemble of atmospheric CO_2 inversions, Biogeosciences, 10, 6699–6720, https://doi.org/10.5194/bg-10-6699-2013, 2013.

Ramonet, M., Ciais,P., Apadula, F., Bartyzel, J., Bastos, A., Bergamaschi, P., Blanc, P. E., Brunner, D., di Torchiarolo, L. C., Calzolari, F., Chen, H., Chmura, L., Colomb, A., Conil, S., Cristofanelli, P., Cuevas, E., Curcoll, R., Delmotte, M., d. Sarra, A., Emmenegger, L., Forster, G., Frumau, A., Gerbig, C., Gheusi, F., Hammer, S., Haszpra, L., Hatakka, J., Hazan, L., Heliasz, M., Henne, S., Hensen, A., Hermansen, O., Keronen, P., Kivi, R., Kominkova, K., Kubistin, D., Laurent, O., Laurila, T., Lavric, J., Lehner, I., Lehtinen, K.E.J., Leskinen, A., Leuenberger, M., Levin, I., Lindauer, M., Lopez, M., Myhre, C. L., Mammarella, I., Manca, G., Manning, A., Marek, M. V., Marklund, P., Martin, D., Meinhardt, F., Mihalopoulos, N., Molder, M., Morgui, J. A., Necki, J., O'Doherty, S., O'Dowd, C., Ottosson, M., Philippon, C., Piacentino, S., Pichon, J. M., Plass-Duelmer, C., Resovsky, A., Rivier, L., Rodó, X., Sha, M.K., Scheeren, H., Sferlazzo, D., Spain, T. G., Stanley, K. M., Steinbacher, M., Trisolano, P., Vermeulen, A., Vítková, G., Weyrauch, D., Xueref-Remy, I., Yala, K., and Yver. Kwok, C.: The fingerprint of the summer 2018 drought in Europe on ground-based atmospheric CO_2 measurements, Philos. T. R. Soc. B, 375, 20190513, https://doi.org/10.1098/rstb.2019.0513, 2020.

Rödenbeck, C., Zaehle, S., Keeling, R., and Heimann, M.: History of El Nino impacts on the global carbon cycle 1957–2016: A quantification from atmospheric CO_2 data, Philos. T. R. Soc. B, 373, 20170303, https://doi.org/10.1098/rstb.2017.0303, 2018a.

Rödenbeck, C., Zaehle, S., Keeling, R., and Heimann, M.: How does the terrestrial carbon exchange respond to interannual climatic variations? A quantification based on atmospheric CO_2 data, Biogeosciences, 15, 2481–2498, https://doi.org/10.5194/bg-15-2481-2018, 2018b.

Santrock, J., Studley, S. A., and Hayes, J. M.: Isotopic analyses based on the mass spectra of carbon dioxide, Anal. Chem., 57, 1444–1448, 1985.

Schilt, A., Baumgartner, M., Schwander, J., Buiron, D., Capron, E., Chappellaz, J., Loulergue, L., Schüpbach, S., Spahni, R., Fischer, H., and Stocker, T. F.: Atmospheric nitrous oxide during the last 140,000 years, Earth Planet. Sci. Lett., 300, 33–43, 2010.

Steele, L.P., Langenfelds, R.L., Krummel, P.B., Van der Schoot, M.V., Spencer, D.A. and Fraser, P.J.: Atmospheric Methane, Carbon Dioxide, Hydrogen, Carbon Monoxide and Nitrous Oxide from Cape Grim Flask Air Samples Analysed by Gas Chromatography in: Baseline Atmospheric Program Australia 2005–2006, edited by: Cainey, J. M., Derek, N., and Krummel, P. B., Australian Bureau of Meteorology and CSIRO Marine and Atmospheric Research, Melbourne, 62–65, https://doi.org/10.4225/08/585c17520427f, 2007.

Tans, P. P., Fung, I. Y., and Takahashi, T.: Observational Constraints on the Global Atmospheric CO_2 Budget, Science, 247, 1431–438, 1990.

Thompson, R. L., Lassaletta, L., Patra, P. K., Wilson, C., Wells, K. C., Gressent, A., Koffi, E. N., Chipperfield, M. P., Winiwarter, W., Davidson, E. A., Tian, H., and Canadell, J. G.: Acceleration of global N_2O emissions seen from two decades of atmospheric inversion, Nat. Clim. Change, 9, 993–998, https://doi.org/10.1038/s41558-019-0613-7, 2019.

Trolier, M., White, J. W. C., Tans, P. P., Masarie, K. A., and Gemery, P. A.: Monitoring the isotopic composition of atmospheric CO_2 measurements from the NOAA Global Air Sampling Network, J. Geophys. Res., 101, 25897–25916, 1996.

Wendeberg, M., Richter, J. M., Rothe, M., and Brand, W. A.: $\delta^{18}O$ anchoring to VPDB: calcite digestion with 18O-adjusted orthophosphoric acid, Rapid Commun. Mass Spectrom., 25, 851–860, https://doi.org/10.1002/rcm.4933, 2011.

Wendeberg, M., Richter, J. M., Rothe, M., and Brand, W. A.: Jena Reference Air Set (JRAS): a multi-point scale anchor for isotope measurements of CO_2 in air, Atmos. Meas. Tech., 6, 817–822, https://doi.org/10.5194/amt-6-817-2013, 2013.

Werner, R. A., Rothe, M., and Brand, W. A.: Extraction of CO_2 from air samples for isotopic analysis and limits to ultra high precision $\delta^{18}O$ determination in CO_2 gas, Rapid Commun. Mass Spectro., 15, 2152–2167, https://doi.org/10.1002/rcm.487, 2001.

WMO Greenhouse Gas Bulletin. The State of Greenhouse Gases in the Atmosphere Based on Global Observations through 2018, Report No 15, 25 November, https://library.wmo.int/index.php?lvl=notice_display&id=21620 (last access: 17 November 2023), 2019.

WMO Greenhouse Gas Bulletin. The State of Greenhouse Gases in the Atmosphere Based on Global Observations through 2021, Report No 18, 26 October, https://library.wmo.int/index.php?lvl=notice_display&id=22149 (last access: 17 November 2023), 2022.

Worthy, D. E. J., Trivett, N. B. A., Hopper, J. F., Bottenheim, J. W., and Levin, I.: Analysis of long-range transport events at Alert, N.W.T., during the Polar Sunrise Experiment, J. Geophys. Res., 99, 25329–25344, 1994.

Zhao, C. L. and Tans, P. P.: Estimating uncertainty of the WMO mole fraction scale for carbon dioxide in air, J. Geophys. Res., 111, D08S09, https://doi.org/10.1029/2005JD006003, 2006.